

Contents lists available at ScienceDirect

Earth-Science Reviews

journal homepage: www.elsevier.com/locate/earscirev



Glacial terminations or glacial interruptions?[★]

Lowell Stott

Dept. Earth Science, University of Southern California, 3651 Trousdale Parkway, Los Angeles, CA 90089, United States of America

ARTICLE INFO

Keywords: Ice Ages Milankovitch theory Carbon Cycle Geologic Carbon Atmospheric CO₂ Hypothesis testing

ABSTRACT

In the early 20th century, after contributing major advances in calculating radiation forcing on planetary bodies, Milutin Milankovitch the Serbian mathematician took up the challenge of explaining why Earth has experienced recurrent episodes of glaciation. Influenced by the ideas of his predecessors, Milankovitch developed a theory that centered on the notion that summertime temperature at high northern latitudes is the most important influence on the advance and retreat of glaciations. The calculations revealed a periodicity in summer insolation that had a reasonable correspondence with what was then known about the occurrence of ice ages. From that was born the elemental foundation of the orbital theory of the ice ages. That theory evolved over the next three decades while retaining the fundamental tenant that summer season insolation at the higher northern latitudes determines Earth's climate variability. Scientists of the day were skeptical, and it was not until the 1960s that new techniques became available to test the temporal predictions of Milankovitch's theory. The orbital theory gained support in the 1950s and 60s when methods for paleoclimate reconstructions documented an orbital-like recurrence pattern of cold and warm climate conditions spanning the past 2.5 million years. Accompanying the documentation of Earth's climate rhythmicity from marine archives have been advances in other areas, including ice core records of atmospheric CO2 that pose challenges to the original orbital theory, namely what role have variations in atmospheric CO₂ played in dictating the transitions from warm to cold and, what caused orbital scale variations in greenhouse gas concentrations? In this contribution we review the current state of knowledge about the Earth's carbon cycle on glacial/interglacial timescales and explore how new information has begun to shed light on the long-standing goal to understand Earth's natural climate rhythmicity. The findings presented here highlight the need to expand research on Earth's geologic processes that influence the carbon budget on glacial timescales. And with this comes a new hypothesis that incorporates geologic processes in orbital scale climate cycles.

1. Introduction

This contribution poses a question that arises from nearly a century of climate research that has sought to understand the factors responsible for some of Earth's most dramatic climate changes. During the Pleistocene were ice ages terminated or were they interrupted? The question may seem subtle at first consideration but as outlined here, the answer to this question would have fundamental implications for understanding the natural climate system behavior that has characterized the Pleistocene. For the past five decades paleoclimate studies that have explored why the Earth's climate underwent large changes during the Pleistocene have characterized two different states, a glaciated state when ice sheets advanced across the northern hemisphere and a second state in which the ice retreated to a minimum and the planet warmed. There have been many studies that demonstrate a natural rhythm to these variations with frequencies like the Earth's orbital cycles, obliquity, precession, and

eccentricity. This rhythmic variability was most clearly demonstrated in proxy records that document a particular aspect of the climate such as temperature that is reflected in the oxygen isotope composition of marine biogenic calcite. Of the many contributions using this proxy the application of oxygen isotope palaeothermometry by Emiliani (1955) and the chronologic constraints used to tie the oxygen isotope variations to Earth's orbital cycles by Broecker (1966) stand out as foundational initial steps. And although the oxygen isotope composition of calcite shells is not a function of temperature alone as Emiliani originally envisioned, it is nonetheless, the most robust recorder of the Pleistocene climate rhythmicity.

Hays et al. (1976) built on those early findings and provided compelling arguments that orbital variations themselves must be the 'pacemaker' to Earth's climate rhythms. By the 1980s the climate community had come to accept that although direct solar forcing due to orbital variations is small, the pacing of climate variations share a

^{*} Stott conceived of the study. Stella Baldwin and Roman Ferraro helped compile the data used in section 2 and assisted with some of the figures.

similar frequency with the orbital cycles and thus, small changes in insolation at high northern latitudes must be the primary driver as Milanković (1957) originally theorized. Other climate feedbacks would somehow amplify the small solar forcing to produce the large shifts from one climate state to the other. In 1986 Imbrie and Imbrie (1986) published the influential book, "Ice ages: solving the mystery" making the case that the breadth of evidence then available was compelling enough to say that the mystery had been solved by showing correspondence in timing between climate changes and orbital variations. But what these scholars did not incorporate into their arguments were the findings by Mercer (1984) who raised questions about the Milankovitch Theory of ice ages by showing glaciers in the southern hemisphere reached a maxima at the same time as northern hemisphere glaciers. Furthermore, the retreat of ice in the southern hemisphere was synchronous with retreat in the northern hemisphere during the last deglaciation. In other words, summer insolation at high northern latitudes by itself would not explain why the southern hemisphere glaciers varied synchronously with those in the northern hemisphere. Mercer went on to point out that atmospheric CO2 was a likely influence on the synchroneity. It took another three decades to acquire enough additional data from the southern hemisphere to firmly establish that Mercer was correct (Clark et al., 2009; Denton et al., 1999; Lowell et al., 1995; Putnam et al., 2013). And by this time, the ice core community had obtained long records of temperature and atmospheric CO2 from Antarctic ice cores that demonstrated a close temporal correspondence between changes in air temperature and changes in atmospheric CO2, that matched the marine oxygen isotope records of ice advance and retreat during the late Pleistocene (Fig. 1).

We now have well resolved reconstructions of temperature, ice volume and atmospheric CO_2 spanning the past 850kyrs (Fig. 1). These records document the timing and the rates of change. Importantly, the temporal pattern of change that is recorded in the ice and in marine records does not share the smoothly varying changes that characterize the orbital insolation cycles. The glaciations during the late Pleistocene spanned about 90 thousand years whereas the transitions to interglacial conditions spanned <10 thousand years. Any hypothesis attempting to explain the temporal history of climate variability vis-à-vis orbital forcing must reconcile why the glaciations were protracted while deglaciations were rapid and short-lived and why CO_2 concentrations share the same temporal characteristics. Explaining the magnitude and temporal phasing of atmospheric CO_2 must be part of the ultimate description of Earth's natural climate behavior.

A case can now be made that in the absence of the greenhouse gas variability affecting the Earth's energy budget the advance and retreat of glaciers would not have been contemporaneous in both hemispheres and the retreat of ice during a deglaciation would not have been so rapid. One way to assess this is to evaluate the radiative effect of changing atmospheric greenhouse gas concentrations during the last glacial maximum (LGM) (Hansen, 2012; Members, 2012). The greenhouse gas portion of the total estimated forcing amounts to $-3 \pm 0.5 \text{ W/m}^2$ of a total -6.5 W/m^2 forcing at the LGM relative to modern. This means that nearly half of the radiative forcing change necessary to explain the \sim 5 °C global mean temperature difference between the Holocene and LGM

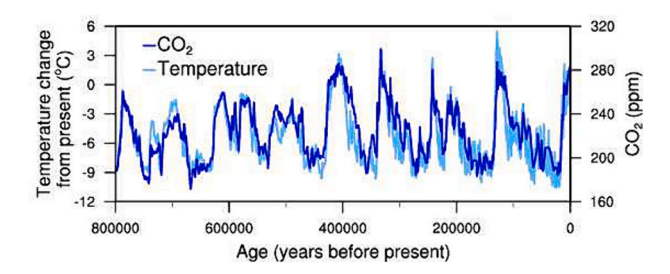


Fig. 1. Atmospheric CO_2 and temperature history from EPICA ice core Antarctica (Luthi et al., 2008).

was due to the reduced greenhouse gases, primarily CO_2 . Hence, without the -3 W/m² from lower greenhouse gas concentrations the total cooling would have been closer to $-2.6\,^{\circ}C$ and the ice in both hemispheres would not have retreated as it did. This is why it is important to ask the question: Are the transitions between the cold and warm states "terminations" or are they "interruptions" caused by transient changes in the carbon budget that released excess CO_2 to the atmosphere that initiated the rapid retreat of glaciers in both hemispheres?

The temporal asymmetry in the 'sawtooth' pattern of atmospheric CO2 has proven as challenging to explain as is the ice sheet variability (Archer, 2010). Urey's original theory (Urey, 1952) that relates atmospheric CO2 removal to weathering and biogeochemical processes, are thought to operate too slowly to have affected the carbon cycle on glacial/interglacial timescales. And the basic theory of weathering feedbacks (Walker et al., 1981) argues that as the climate cools chemical weathering rates should decrease thereby reducing the flux of alkalinity to the oceans that would limit the amount of CO2 removed from the atmosphere. The concept of a temperature feedback in the carbon cycle has been championed in various attempts to explain the long-term evolution of the Earth's climate and carbon system (Berner and Caldeira, 1997; Berner et al., 1983). But this climate-CO₂ feedback has also been challenged on the basis of observations that document similar weathering fluxes in both cold, glaciated environments and in tropical regions (Edmond and Huh, 1997). The argument is that frost action combined with glacial erosion constantly removes weathered surfaces, providing new substrate for weathering.

Perhaps the most striking example of the climate feedback conundrum is the long-term Cenozoic cooling that coincided with the uplift of the Himalayan mountains. Raymo et al. (1988) and Raymo and Ruddiman (1992) pointed to the record of increasing ⁸⁷Sr during the mid to late Cenozoic as evidence that the uplift was accompanied by increased weathering of the uplifted terrane, which they argue led to a drawdown of atmospheric CO2 and global cooling. Broecker and Sanyal (1998) argued instead that the ⁸⁷Sr record could not, by itself be used to argue for increased weathering rates over the Cenozoic because the uplift and exposure of Sr-rich terrane could explain the Cenozoic record of increasing ⁸⁷Sr without an increase in weathering rates. But more recently, Misra and Froelich (2012) produced a Cenozoic record of marine ⁷Li that documents a long-term increase over the Cenozoic that is taken to represent increased denudation under increasingly glaciated climate conditions and increased incongruent chemical weathering. So, on a million-year time scale, when there are terranes to be physically and/or glacially eroded, it appears that climate cooling is not a limiting

Several studies have investigated whether weathering rates could have varied over the Pleistocene. Zeebe and Caldeira (2008) used an isotope mass balance approach to explore whether weathering feedbacks influenced the mean atmospheric CO2 over the entire Pleistocene. They found a small trend over the Pleistocene, concluding there was not much evidence in the isotope record to assert that weathering rates fundamentally changed. But their approach was unable to resolve whether there were changes in weathering on glacial/interglacial timescales. Other studies using isotope systems to investigate chemical weathering rates between the present and last glacial maximum found no net change in weathering (Foster and Vance, 2006). Similar findings have been found using biogeochemical models to simulate continental weathering during periods of sea level low stand (Munhoven, 2002) or earth system models to simulate an entire glacial cycle and CO₂ history (Wallmann et al., 2016). These studies argue that reduced continental chemical weathering during glaciations would have been roughly balanced by increased weathering of exposed shelves during low stands of sea level. There are uncertainties and assumptions built into each approach. We don't have direct estimates of weathering rates from exposed shelves as sea level fell. And importantly, these studies put no constraint on the fluxes of carbon into the surface environment (ocean/ atm) from geologic sources throughout the Pleistocene. These fluxes are

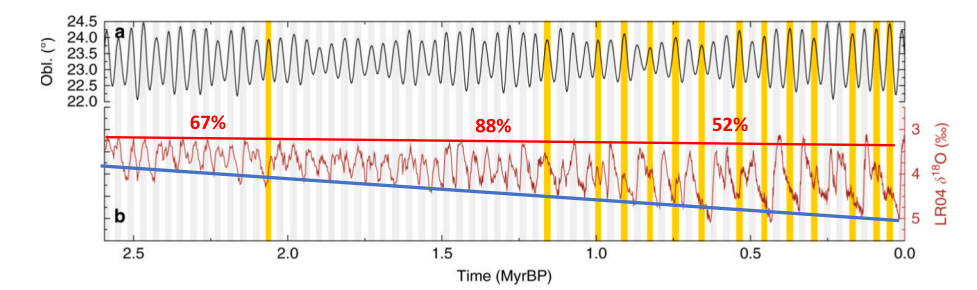


Fig. 2. Figure from Köhler and van de Wal., (2020). Red and blue lines added here. The percentages of interglacials that did not coincide with obliquity maxima during the early, mid, and late Pleistocene are shown above the red line. Note that the magnitude of interglacial d¹⁸O values (red line) has not varied significantly over the Pleistocene whereas the magnitude of the glacial maximum values (blue line) has become progressively larger. (For interpretation of the references to colour in this figure legend, the reader is referred to the web version of this article.)

presumed constant. For example, this is an explicit assertion in the most recent Paleoclimate Model Intercomparison Project (PMIP) experiments using Earth System Models that attempted to simulate lower atmospheric CO₂ during the LGM (Lhardy et al., 2021). The results of those model experiments are striking because models with freely varying atmospheric CO₂ simulate higher atmospheric CO₂ rather than lower atmospheric CO₂ under glacial boundary conditions. The models all simulate greater carbon storage in the ocean but in order to simulate LGM atmospheric CO₂ values similar to that observed from ice cores, the models require an "alkalinity adjustment" without which CO₂ reaches as high as 434 ppm. It is evident from these results that there is a need to put better constraints on riverine fluxes and carbon burial during glaciations as well as geologic emissions of carbon.

At the present time we have no direct estimates of carbon emissions from marine or subaerial sources during glaciations. It's therefore impossible to say whether the carbon cycle maintained an equilibrium balance of inputs and outputs. Indeed, the premise of the current paper is that the carbon fluxes into and out of the reactive zone are not in complete balance most of the time. Instead, the carbon output fluxes (consumption of carbon and carbon burial) outpace the carbon input fluxes, except during an interruption when excess carbon is released to the ocean/atm from geologic sources.

A further motivation for considering the possibility that the carbon cycle has not been in balance during glacial/interglacial cycles is the observation that the climate as a whole has become progressively colder, and the size of ice sheets have become progressively larger over the past 2.5 million years (Fig. 2). The interglacial state as reflected in the oxygen isotope record (Lisiecki and Raymo, 2005) has remained effectively unchanged. But the glacial values have become progressively larger, reflecting an increase in the magnitude of glaciations and colder temperatures (Fig. 2). This is indicative of a long-term decrease in the Earth's net energy budget. In fact, the Pleistocene trend can be considered a continuation of the longer-term cooling trend since the late Miocene.

2. Hypothesis

With the above background in mind, the following new hypothesis is presented:

2.1. Glaciation is the preferred state of the climate system and has been for much of the late Cenozoic

- A glaciated climate state is self-perpetuating in the absence of "Interruptions" that cause the climate to warm rapidly and temporarily.
- Erosion, weathering, and carbon burial have led to a net removal of carbon from the reactive zone for most of the mid to late Cenozoic.
- Glacial interruptions occur when geologic carbon reservoirs are disturbed and release excess carbon to the reactive zone.

- Carbon reservoirs can be disturbed when increased ice volume reduces hydrostatic pressure on hydrate caps that otherwise keep geologic carbon reservoirs from leaking and affect changes in the flux of carbon from the mantle to volcanic sources, including mid ocean ridges.
- A release of excess geologic carbon to the ocean/atm leads to rapid warming and ice retreat in both hemispheres but is transient because the carbon system immediately begins to compensate for the added carbon.
- The link between an interruption and Earth's orbital variability is the time required to compensate for the release of excess carbon and to rebuild ice cover.

It is important to emphasize this paper poses a question that motivates this hypothesis. This paper does not answer the question, nor does it validate the hypothesis. However, there is enough evidence now available to begin to assess whether this hypothesis should be rejected or should be investigated further.

The hypothesis set forth here makes specific predictions that run counter to predictions required by the prevailing hypothesis that attempts to explain variations in atmospheric CO₂ that accompanied glacial/interglacial cycles with ocean-only processes.

2.2. Predictions to be examined

The prevailing hypothesis to explain the glacial-to-interglacial changes in atmospheric CO2 can be viewed as an "ocean-only model" because in this model the total inventory of carbon in the reactive zone is considered constant. The only thing that changes between a glacial climate and a warm interglacial climate is that the ocean sequesters carbon from the atmosphere and keeps it isolated in the deep sea as the climate cools and ice advances. The atmospheric carbon is transferred to the deep sea thermodynamically and biologically and is thought to accumulate primarily as respired metabolic carbon in the deep sea (Anderson et al., 2019; Jacobel et al., 2020; Sigman et al., 2010; Skinner et al., 2015; Toggweiler et al., 2003a; Toggweiler et al., 2003b; Yu et al., 2010). To keep the excess respired carbon from ventilating the prevailing hypothesis also requires a change in mean overturning rate of the oceans until the end of an ice age when excess metabolic carbon is released rapidly from the deep sea to the atmosphere. The reasoning behind this hypothesis is logical. The oceans are the largest reactive pool of carbon with over 38,000Gt of carbon whereas the atmosphere has less than 800Gt of carbon. Thermodynamics and biological processes combine with ocean dynamics to regulate the concentration of CO2 in the modern atmosphere on time scales of the overturning of deep water, ~1000 years (Broecker and Sanyal, 1998). This is a relatively short time scale in the context of a glacial/interglacial cycle. But altering the turnover rate and affecting the transfer of carbon from the atmosphere to the deep sea via biological pumping and thermodynamic exchange might explain the drop in atmospheric CO2 during glaciations if all aspects work in unison. It is prudent therefore to thoroughly evaluate whether an ocean-only hypothesis can be validated by observations. Indeed, there have been numerous efforts to test the ocean-only hypothesis. But the recent availability of global datasets of proxy variables makes it possible to evaluate the ocean-only model more critically.

A description of the major elements of the ocean-only model can be found in the paper by Barker and Knorr (2021). One of the critical elements of the ocean-only model is the presumption that ice sheets in the northern hemisphere reach a critical size that renders them unstable and thereby susceptible to rapid collapse and retreat in response to a modest change in insolation forcing as prescribed by the Milankovitch theory. Again, this would not explain the fact the southern hemisphere glaciers retreated simultaneously with those in the northern hemisphere. And in the ocean-only model rising atmospheric CO₂ during a deglaciation is a consequence of changing ocean processes that release respired carbon to the atmosphere. In this way CO2 sequestration and release from the ocean are feedbacks rather than a primary forcing. This too makes specific predictions that should be evaluated against observations. The argument put forth in this paper is that CO₂ is a primary forcing and its linkage to orbital time scale variability is through ice sheet imposed hydrostatic pressure changes that affect the stability of deep and near surface reservoirs of geologic carbon that can be released to the ocean/

The following is a set of predictions that the prevailing ocean-only hypothesis makes, each of which is evaluated more thoroughly with new compilations of palaeoceanographic data that include observations from each of the ocean basins. These compilations make it possible to evaluate which records provide well-resolved observations and which records lack sufficient resolution or are compromised in some way and should not be included in hypothesis testing. This is a major step forward (Muglia et al., 2023; Mulitza et al., 2021; Rafter et al., 2022).

2.3. Prediction 1: Metabolic carbon sequestered in the deep ocean during glaciations would increase the surface to deep water $\delta^{13}C$ gradient

Because marine phytoplankton produce organic matter whose δ^{13} C is ~20% lower than that of dissolved carbon in the surface ocean, the oxidation and transfer of organic carbon into dissolved carbon stored in the deep sea shifts the deep ocean DIC δ^{13} C values lower relative to the surface ocean. If the prevailing hypothesis is correct the $\delta^{13}C$ difference between the surface and deep ocean should have been larger during a glacial when atmospheric CO2 was low because excess respired organic carbon would have been transferred to the deep ocean and kept away from the atmosphere. Such a shift in the vertical δ^{13} C gradient would be recorded in the calcite shells of foraminifera. Planktic foraminifera secrete calcite from dissolved carbon in the surface ocean while benthic foraminifera record deep water $\delta^{13}\text{C}$ values. These proxy records exist for much of the global ocean (Mulitza et al., 2021). If the ocean-only model is correct the $\delta^{13}C$ gradient between the planktic and benthic foraminifera increased to a maximum at the time of lowest atmospheric CO₂, the glacial maximum. On the other hand, if the ocean only model is not correct and excess respired carbon did not accumulate in the deep sea, the $\delta^{13}\text{C}$ gradient between the surface and deep ocean would not be significantly different than in the modern or late Holocene Ocean. This prediction is evaluated here by comparing planktic and benthic $\delta^{13}C$ data from the late Holocene and Last Glacial Maximum (LGM) taken from marine sediment cores.

We also expect small changes in the global ocean $\delta^{13}C$ due to the transfer of terrestrial organic carbon to the oceans as ice sheets advanced and denuded the landscape during glaciations (Peterson et al., 2014; Shackleton, 1977) or changes in the ratio of organic to in organic carbon burial as sea level fell (Cartapanis et al., 2018; Wallmann et al., 2016). Both factors would have affected the surface and deep sea equally and thus would not have changed the surface to deep water $\delta^{13}C$ gradient at the glacial maximum.

We evaluated the benthic and planktic foraminiferal $\delta^{18}O$ and $\delta^{13}C$

data (Mulitza et al., 2021) using PaleoDataView (Langner and Mulitza, 2019). We culled the database for carbon isotope results for the planktic Globigerinoids ruber (white) from the Atlantic, Pacific and Indian Ocean basins, isolating values from the late Holocene and the LGM. We similarly culled the database for benthic Cibicidoides wuellerstorfi, Cibicidoides mundula and Cibicidoides spp. data from the Pacific, Atlantic and Indian Oceans. We are specifically evaluating the *magnitude* of change in δ^{13} C ($\Delta\delta^{13}$ C) between the late Holocene and last glacial maximum (LGM) of the tropical surface-dwelling G. ruber because the calcite of this for aminifer records changes in the $\delta^{13} C$ of surface waters in contact with the atmosphere (Kawahata, 2005; Lin et al., 2004; Numberger et al., 2009) with a species-specific offset of 0.9% for specimens between 250 and 350 mm (Spero et al., 2003). With a species-specific offset of 0.9% the late Holocene G. ruber records a late Holocene $\delta^{13}C_{DIC}$ value close to 2.1‰, very close to the modern, preindustrial value. Köhler and Mulitza (2023) find no evidence of a carbonate ion influence in down core records of G. ruber $\delta^{18}O$ and $\delta^{13}C$ compared to model simulated surface ocean δ^{13} C over the past 160ky. We use the δ^{13} C of C. wuellerstorfi, Cibicidoides mundula and Cibicidoides spp., epibenthic species from marine sediment cores from depths below 1500 m in the Pacific and Indian Ocean because this benthic group has been shown to record the δ^{13} C of bottom water δ^{13} C DIC (Schmittner et al., 2017). There are small effects due to carbonate ion and pressure differences, but these are small and do not affect the $\Delta\delta^{13}$ C estimate (LGM-Holocene difference) considered here. We exclude the Atlantic benthic records for the estimate because changes in water mass distributions in that basin during the LGM complicate a Holocene -LGM difference calculation. Furthermore, the deep Pacific is the largest deep-water reservoir for carbon. It contains the highest concentrations of dissolved inorganic carbon due to the accumulation of respired carbon and is also the primary source of carbon released back to the atmosphere via the Southern Ocean (Chen et al., 2022; Prend et al., 2022). Nonetheless the Atlantic data estimates are given in Table 2.

Many cores in the database are of very low temporal resolution due to low sediment accumulation rates. Cores were excluded from analysis if the oxygen isotope stratigraphy could not be used to resolve a clear late Holocene and LGM interval. Some cores contain a well resolved LGM section but are missing the late Holocene presumably because of coring disturbances. Some, but not all cores have radiocarbon ages to assist in delimiting the late Holocene and LGM. A significant number of core records are simply too noisy to provide a definitive cutoff for the LGM (23-18kyBP) and the late Holocene (5-0kyBP) based on the oxygen isotope stratigraphies. This is likely a consequence of very low sediment accumulation rates and bioturbation that mixes the sediment. We also avoided cores in which there were less than three isotope values for the late Holocene or LGM sections. The reason for this is that all cores exhibit some variance in both $\delta^{18} O$ and $\delta^{13} C$ so an effort was made to include enough (at least 3) values to provide an average rather than a single value for either interval. The cores included in the analysis are provided in Tables 1 and 2. The cores excluded from the analysis are summarized in the supplemental tables (S Table 1, S Table 2). Fig. 3 shows the distribution of cores used in the analysis.

We begin by summarizing the *G. ruber* results from each of the three ocean basins. There are 29 core records from the tropical Pacific, 15 from the tropical Atlantic and 19 from the tropical Indian Ocean (Fig. 3). Fig. 4 displays the difference between the late Holocene and LGM for cores from each basin. The values vary between -1 and -0.1%. However, most values fall between -0.5 and -0.3%. There is no clear indication that values from one ocean basin are significantly offset from another basin. Nonetheless, a *t*-test was used to assess whether this inference is statistically valid. The results of these two tailed *t*-tests are summarized in Table 3. We find no statistically significant difference between the mean values in each basin at the 95% confidence level. The population average and median from each basin is depicted in the whisker plots from each basin in Fig. 5. The average value for each ocean is -0.4% very similar to the estimated mean global ocean shift from the

Table 1 G. ruber LGM-Holocene δ^{13} C difference.

Pacific Core	Depth (m)	Latitude	Longitude	G. ruber δ ¹³ C ‰
FR01_97-12	991	-23.669	154.028	-0.2
MD05-2896	1477	8.825	-111.441	-0.2
MD05-2925	1661	-9.34	151.46	-0.4
GIK17940-2	1727	20.117	117.383	-0.5
VM28-235	1746	-5.5	160.5	-0.1
VM24-150	1849	-2.2	155.7	-0.4
MD98-2181	2114	6.5	125.82	-0.3
RC8-102	2180	-1.417	-86.85	-0.3
RC13-140	2246	2.867	-87.75	-0.6
MD9109-15GGC	2311	-0.023	158.941	-0.1
RC11-238	2573	-1.517	-85.817	-0.3
V19-28	2720	-2.367	-84.65	-0.5
ML1208-20BB	2850	1.27	-157.26	-0.4
ML 12088-17PC	2926	0.48	-156.45	-0.3
ML 1208-12GC	3050	-0.22	-155.96	-0.4
ML1208-28BB	3153	2.97	-159.2	-0.3
SO26_58ka	3200	2.728	-95.188	-0.5
PLDS 7G	3253	-3.338	-102.453	-0.5
ML1208 18GC	3362	0.59	-159.66	-0.2
ODP769	3656	8.785	121.295	-0.4
AVERAGE				-0.4
ST. DEV.				0.1

Atlantic core	Depth (m)	Latitude	Longitude	G. ruber δ^{13} C ‰
GeoB6518-1	962	-5.588	11.222	-0.3
GeoB2107-3	1048	-27.177	-46.452	-0.3
GeoB16202-2	2248	-1.908	-41.592	-0.6
ODP658C	2273	20.749	-18.581	-0.2
MD02-2594	2440	-34.71	17.338	-0.3
GeoB2004-2	2569	-30.87	14.343	-0.5
GEOFARKF13	2690	37.578	-31.842	-0.5
GIK13291-1	2696	18.053	-18.067	-0.5
GIK16771-2	2764	0.817	-15.51	-0.6
GeoB1903-3	3161	-8.675	-11.845	-0.5
Geo5115-2	3291	-24.143	-14.043	-0.5
GeoB2016-1	3385	-31.9	-1.33	-0.1
Geo5121-2	3486	-24.183	-12.022	-0.4
GeoB9624-1	3894	20.511	-20.659	-0.8
GeoB3801-6	4546	-29.512	-8.305	-0.3
GIK16773-1	4662	-0.972	-9.443	-0.7
AVERAGE				-0.4
STD DEV				0.2

Indian core	Depth (m)	Latitude	Longitude	G. ruber δ ¹³ C ‰
M74_4_1096-1	328	4.262	73.246	-0.2
GeoB12615-4	446	-7.138	39.841	-0.4
SO189-144KL	481	1.155	98.066	-0.3
SO189-39KL	517	-0.79	99.909	-0.2
RC09-166	738	12.15	44.4	-1
SO189-119KL	808	3.518	96.314	-0.2
MD98-2170	832	-10.59	125.39	-0.2
MD76-131	1230	15.53	72.568	-0.3
GeoB10069-3	1250	-9.595	120.917	-0.3
GIK16160-3	1339	-18.24	37.87	-0.3
GeoB10053-7	1372	-8.677	112.872	-0.4
GeoB9311-1	1407	-21.552	36.413	-0.4
M1_143KK	1522	1.25	44.783	-0.4
GeoB10038-4	1891	-5.938	103.246	-0.2
MD76-135	1895	14.433	50.518	-0.5
GeoB3005-1	2316	14.972	54.37	-0.6
M31_3_KL35	2330	14.972	54.37	-0.7
MD77-202	2427	19.222	60.682	-0.6
SO42-74KL	3212	14.321	57.347	-0.6
M1_114KK	3843	8.008	51.213	-0.4
AVERAGE				-0.4
STD DEV				0.2

Table 2 Cibicidoides LGM-Holocene δ^{13} C difference.

Pacific Core	Depth (m)	Latitude	Longitude	<i>C.</i> spp. δ ¹³ C ‰
MD05-2896	1477	8.825	-111.441	-0.3
MD97-2151	1598	8.728	109.869	-0.4
GIK17961-2	1795	8.5	-112.332	-0.4
SO213_2_82-1	2066	-45.778	176.602	-0.4
MD05-2904	2066	19.455	116.253	-0.5
MD98-2181	2114	6.5	125.82	-0.4
MD9109-15GGC	2311	-0.023	158.941	-0.4
RR0503_125JPC	2541	-36.2	176.89	-0.8
HYIV2015-B9	2603	10.248	112.732	-0.4
TR163-25 T	2650	-1.65	-88.45	-0.4
ML1208-28BB	3153	2.97	-159.2	-0.6
SO26_58ka	3200	2.728	-95.188	-0.5
H214	3300	-36.93	177.44	-0.4
Vi 37GC	3300	50.42	167.732	-0.7
ML1208-18GC	3362	0.59	-159.66	-0.4
SO26_131KA	3381	3.527	-85.003	-0.5
MW9109-48GGC	3397	-0.075	161.003	-0.5
MD02-2489	3640	54.391	-148.921	-0.6
AVERAGE				-0.5
ST. DEV.				0.1

GeoB2107-3 1048 -27.177 -46.452 -0.8 SAN-76 1682 -24.43 -42.28 -0.2 GeoB16202-2 2248 -1.908 -41.592 -0.9 ODP658C 2273 20.749 -18.581 -0.2 GeoB2004-2 2569 -30.87 14.343 -0.9 GEOFARKF13 2690 37.578 -31.842 -0.3 GIK16771-2 2764 0.817 -15.51 -0.6 GeoB1903-3 3161 -8.675 -11.845 -0.7 Geo5115-2 3291 -24.143 -14.043 -0.5 GeoB2016-1 3385 -31.9 -1.33 -0.3 Geo5121-2 3486 -24.183 -12.022 -0.4 GeoB3801-6 4546 -29.512 -8.305 -0.6 GIK16773-1 4662 -0.972 -9.443 -0.5 AVERAGE -0.5 ST. DEV. 0.2	Atlantic Core	Depth (m)	Latitude	Longitude	C. spp. δ^{13} C ‰
GeoB16202-2 2248 -1.908 -41.592 -0.9 ODP658C 2273 20.749 -18.581 -0.2 GeoB2004-2 2569 -30.87 14.343 -0.9 GEOFARKF13 2690 37.578 -31.842 -0.3 GIK16771-2 2764 0.817 -15.51 -0.6 GeoB1903-3 3161 -8.675 -11.845 -0.7 Geo5115-2 3291 -24.143 -14.043 -0.5 GeoB2016-1 3385 -31.9 -1.33 -0.3 Geo5121-2 3486 -24.183 -12.022 -0.4 GeoB3801-6 4546 -29.512 -8.305 -0.6 GIK16773-1 4662 -0.972 -9.443 -0.5 AVERAGE -0.5	GeoB2107-3	1048	-27.177	-46.452	-0.8
ODP658C 2273 20.749 -18.581 -0.2 GeoB2004-2 2569 -30.87 14.343 -0.9 GEOFARKF13 2690 37.578 -31.842 -0.3 GIK16771-2 2764 0.817 -15.51 -0.6 GeoB1903-3 3161 -8.675 -11.845 -0.7 Geo5115-2 3291 -24.143 -14.043 -0.5 GeoB2016-1 3385 -31.9 -1.33 -0.3 Geo5121-2 3486 -24.183 -12.022 -0.4 GeoB3801-6 4546 -29.512 -8.305 -0.6 GIK16773-1 4662 -0.972 -9.443 -0.5 AVERAGE -0.5	SAN-76	1682	-24.43	-42.28	-0.2
GeoB2004–2 2569 -30.87 14.343 -0.9 GEOFARKF13 2690 37.578 -31.842 -0.3 GIK16771–2 2764 0.817 -15.51 -0.6 GeoB1903–3 3161 -8.675 -11.845 -0.7 Geo5115–2 3291 -24.143 -14.043 -0.5 GeoB2016–1 3385 -31.9 -1.33 -0.3 Geo5121–2 3486 -24.183 -12.022 -0.4 GeoB3801–6 4546 -29.512 -8.305 -0.6 GIK16773–1 4662 -0.972 -9.443 -0.5 AVERAGE -0.5	GeoB16202-2	2248	-1.908	-41.592	-0.9
GEOFARKF13 2690 37.578 -31.842 -0.3 GIK16771-2 2764 0.817 -15.51 -0.6 GeoB1903-3 3161 -8.675 -11.845 -0.7 Geo5115-2 3291 -24.143 -14.043 -0.5 GeoB2016-1 3385 -31.9 -1.33 -0.3 Geo5121-2 3486 -24.183 -12.022 -0.4 GeoB3801-6 4546 -29.512 -8.305 -0.6 GIK16773-1 4662 -0.972 -9.443 -0.5 AVERAGE -0.5	ODP658C	2273	20.749	-18.581	-0.2
GIK16771–2 2764 0.817 -15.51 -0.6 GeoB1903–3 3161 -8.675 -11.845 -0.7 Geo5115–2 3291 -24.143 -14.043 -0.5 GeoB2016–1 3385 -31.9 -1.33 -0.3 Geo5121–2 3486 -24.183 -12.022 -0.4 GeoB3801-6 4546 -29.512 -8.305 -0.6 GIK16773–1 4662 -0.972 -9.443 -0.5 AVERAGE -0.5	GeoB2004-2	2569	-30.87	14.343	-0.9
GeoB1903-3 3161 -8.675 -11.845 -0.7 Geo5115-2 3291 -24.143 -14.043 -0.5 GeoB2016-1 3385 -31.9 -1.33 -0.3 Geo5121-2 3486 -24.183 -12.022 -0.4 GeoB3801-6 4546 -29.512 -8.305 -0.6 GIK16773-1 4662 -0.972 -9.443 -0.5 AVERAGE -0.5	GEOFARKF13	2690	37.578	-31.842	-0.3
Geo5115-2 3291 -24.143 -14.043 -0.5 GeoB2016-1 3385 -31.9 -1.33 -0.3 Geo5121-2 3486 -24.183 -12.022 -0.4 GeoB3801-6 4546 -29.512 -8.305 -0.6 GIK16773-1 4662 -0.972 -9.443 -0.5 AVERAGE -0.5	GIK16771-2	2764	0.817	-15.51	-0.6
GeoB2016-1 3385 -31.9 -1.33 -0.3 Geo5121-2 3486 -24.183 -12.022 -0.4 GeoB3801-6 4546 -29.512 -8.305 -0.6 GIK16773-1 4662 -0.972 -9.443 -0.5 AVERAGE -0.5	GeoB1903-3	3161	-8.675	-11.845	-0.7
Geo5121-2 3486 -24.183 -12.022 -0.4 GeoB3801-6 4546 -29.512 -8.305 -0.6 GIK16773-1 4662 -0.972 -9.443 -0.5 AVERAGE -0.5	Geo5115-2	3291	-24.143	-14.043	-0.5
GeoB3801–6 4546 –29.512 –8.305 –0.6 GIK16773–1 4662 –0.972 –9.443 –0.5 AVERAGE –0.5	GeoB2016-1	3385	-31.9	-1.33	-0.3
GIK16773–1 4662 –0.972 –9.443 –0.5 AVERAGE –0.5	Geo5121-2	3486	-24.183	-12.022	-0.4
AVERAGE -0.5	GeoB3801-6	4546	-29.512	-8.305	-0.6
	GIK16773-1	4662	-0.972	-9.443	-0.5
ST. DEV. 0.2	AVERAGE				-0.5
	ST. DEV.				0.2

Indian Core	Depth (m)	Latitude	Longitude	C. spp. δ ¹³ C
MD76-125	1877	8.35	75.2	-0.4
GeoB10038-4	1891	-5.938	103.246	-0.4
MD76-135	1895	14.433	50.518	-0.5
SO42-74KL	3212	14.321	57.347	-0.5
AVERAGE				-0.5
ST. DEV				0.1

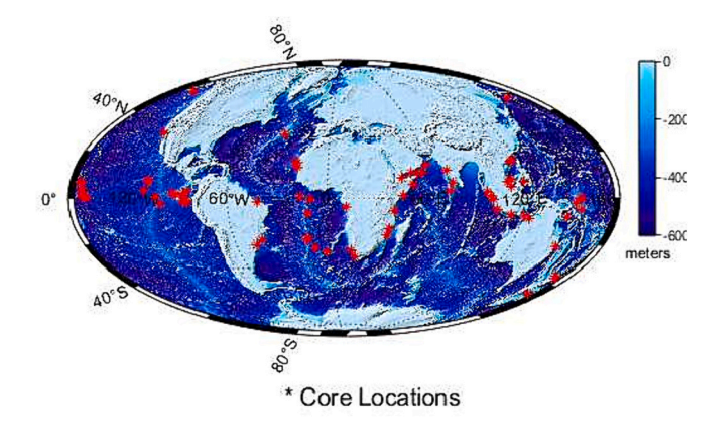


Fig. 3. Topographic map depicts the locations of cores (red stars) from which *G. ruber* and *Cibicidoides* δ^{13} C data were obtained. (For interpretation of the references to colour in this figure legend, the reader is referred to the web version of this article.)

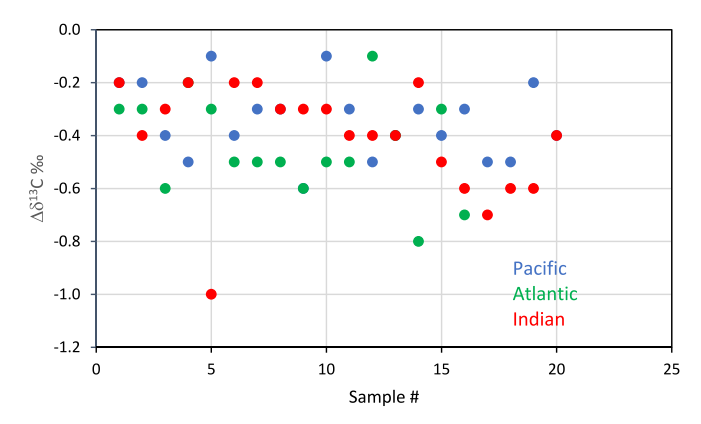


Fig. 4. LGM-Holocene $\Delta \delta^{13}$ C of *G. ruber* from each ocean basin.

Table 3 t-test results of *G. ruber* intercomparisons.

	Pacific vs Atlantic	Atlantic vs Indian	Pacific vs Indian
ci	[-0.0585;0.1776]	[-0.1014;0.1689]	[-0.1457;0.0942]
h	0.0	0.0	0.0
p	0.3	0.6	0.7
tstat	1.0	0.5	0.4
df	33.0	34.0	37.0
sd	0.2	0.2	0.2

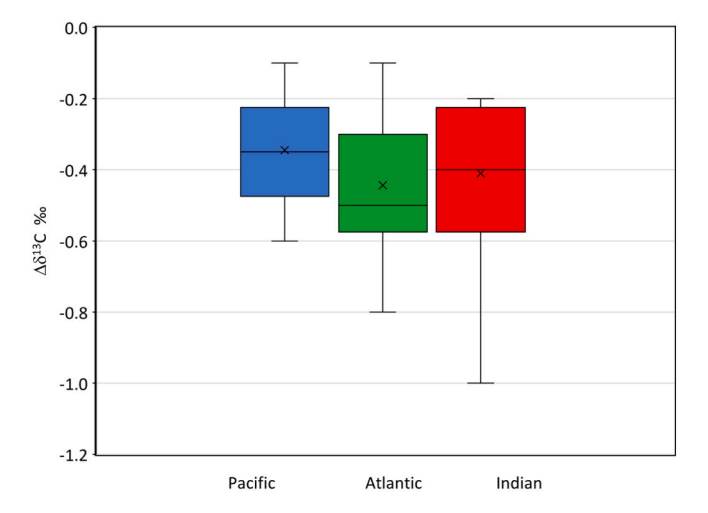


Fig. 5. Whisker plots of the *G. ruber* LGM-Holocene $\Delta\delta^{13}$ C values for each ocean basin.

Holocene to LGM compiled by Peterson et al. (2014). Note that we limit the depiction of $\Delta\delta^{13}C$ values to one decimal place.

The Cibicidoides $\Delta \delta^{13}$ C data are presented by depth in Fig. 6. As with the *G. ruber* data, the values have a large range, but most values are between -0.4 to -0.5% and thus the same as the *G. ruber* results. The mean for the entire group of cores is -0.5% in both the Indian and Pacific. There is no apparent distinction between the North and South Pacific

There are four values from the Pacific that are more negative than the rest. Two of the cores have values of -0.6 ‰. These are from locations near other cores in the dataset with smaller $\Delta\delta^{13}C$ values close to the population mean (less negative values). Core ML1208-28BB for example is from 3153 m water depth in the central equatorial Pacific. For this core there were three to four replicates for each LGM sample. The replicate *Cibicidoides* $\delta^{13}C$ values range between -0.4 to -0.2‰. Hence, the actual Holocene-LGM difference is not tightly constrained for this

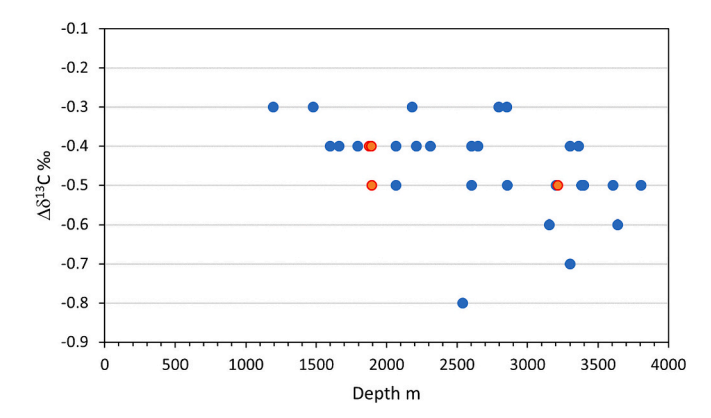


Fig. 6. Cibicidoides LGM-Holocene $\Delta\delta^{13}$ C values for the Pacific (blue) and Indian Ocean (red) as a function of water depth. (For interpretation of the references to colour in this figure legend, the reader is referred to the web version of this article.)

low sedimentation rate core that likely suffers from bioturbation effects.

Because there are several values with lower $\Delta\delta^{13}C$ values among deeper water cores we applied another one tailed t-test to evaluate whether the values above 2500 m water depth are statistically distinct from those below 2500 m (Table 4). The null hypothesis, that the values are statistically the same, was not validated by this test. However, the probability of this outcome is low, primarily because of the relatively small sample size and because we're trying to distinguish between differences on the order of 0.1%. So, while the deeper water sites may have a larger LGM-Holocene $\Delta \delta^{13}$ C, the difference is insignificant in the context of assessing whether there was an increase in the surface to deep water gradient as the prevailing hypothesis predicts. One can see from the whisker plots (Fig. 7) that the population values are the same as those for *G. ruber*. The average LGM-Holocene is -0.5% for the Pacific and Indian Ocean. It is the same for the Atlantic as well (S. Table 2). We find from this analysis that the prevailing hypothesis fails this test. The surface to deep water δ^{13} C gradient was not larger during the LGM in either the Pacific or Indian Ocean.

Having tested this prediction, it is important to emphasize that this finding does not negate changes in upwelling and ocean circulation change that can influence exchange of CO₂ with the atmosphere (Anderson et al., 2009; Burke and Robinson, 2011). But evidence of changing upwelling does not directly reflect how much respired carbon was stored in the deep ocean during the LGM or how much carbon was being upwelled to the surface during the deglaciation. The $\delta^{13} C$ data do not support the notion that there were increased quantities of respired carbon stored in the deep sea during the LGM or that excess carbon was ventilated during the last deglaciation.

2.4. Prediction 2: Carbon sequestration in the deep sea requires longer residence times

The ocean-only model envisions excess respired carbon accumulating in a deep ocean reservoir during a glaciation. To accomplish this, the biological pump converts CO_2 in the surface ocean to organic matter that is then oxidized and respired as it passes to the deep ocean. This

Table 4 t-test results of *Cibicidoides* intercomparisons.

	Deep vs Intermediate
ci	[-Inf;-0.008]
h	1
p	0.0381
tstat	-1.8695
df	20.0
sd	0.1

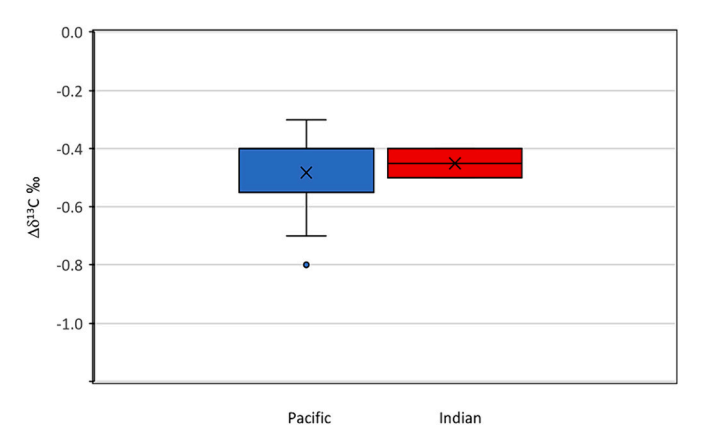


Fig. 7. Whisker plot of *Cibicidoides* LGM-Holocene $\Delta\delta^{13}$ C values for each the deep Pacific (blue) and Indian (red) oceans. (For interpretation of the references to colour in this figure legend, the reader is referred to the web version of this article.)

process may have been more efficient in producing and transferring metabolic carbon to the deep-sea during glaciations, particularly in regions that are today iron limited (Martin, 1990). But to be effective at lowering atmospheric CO_2 over a glacial cycle the excess respired carbon must remain isolated from the atmosphere. Therefore, to explain the long, $\sim 90 \mathrm{kyr}$ long decline in atmospheric CO_2 during a glaciation a biological pump mechanism must be coupled to progressive decrease in the rate of ventilation of the deep-sea so that less and less respired carbon escapes back to the atmosphere during a glaciation. This is a major challenge for the ocean-only model because the ventilation of the deep sea cannot slow too much, or the deep sea would become anoxic.

There is now a global data base of radiocarbon measurements from benthic foraminifera taken from cores throughout the global ocean (Rafter et al., 2022). These can be used to estimate the ventilation age of deep waters in the glacial ocean (Rafter et al., 2022). The radiocarbon ventilation ages for the deep ocean extend to about 30kyBP, the end of the last ice age. This data cannot be used to assess whether there was a long-term decline in ventilation rates over the entire glaciation. Nonetheless, the ocean only hypothesis predicts that the ventilation rate of the deep ocean was lowest during the LGM (23-18kyBP). This is tested by evaluating the ventilation age estimates from radiocarbon dates of benthic foraminifera for the last glacial maximum, comparing those estimates with modern ventilation ages. If the ocean-only model is not correct, there should be no substantial increase in the ventilation age of deep waters, particularly in the Pacific, the largest ocean reservoir where the oldest and most carbon-rich waters accumulate.

In the modern Pacific Ocean, the ¹⁴C ventilation age of abyssal water formed in the Southern Ocean increases as it flows toward the North Pacific. This aging is captured in the radiocarbon activity (Δ^{14} C) of dissolved inorganic carbon (Fig. 8). The Δ^{14} C values of abyssal waters in the Pacific below 1500 m exhibit a small amount of variance at any given latitude (Fig. 8). This variance stems from analytical uncertainty in the measurements itself, which is typically measured in units of 10s of years and the natural aging (loss of radiocarbon) of waters that have been isolated from the atmosphere. In the modern ocean the deep waters in the deep Pacific are between about 1300 and 2200 ¹⁴C years older the preindustrial atmosphere. Abyssal waters at around 30°S are about 1800 years older than the preindustrial atmosphere whereas the abyssal waters around 30°N are about 2200 years older than the preindustrial atmosphere (Fig. 8). There is also a longitudinal gradient with oldest waters in the northeast Pacific (Matsumoto, 2007). The dispersion of ages throughout the abyssal North Pacific is ~400 years. An equally important observation is that as abyssal waters in the North Pacific age, they lose oxygen via metabolic respiration. In fact, there is a direct relationship between the aging of these waters, as measured in

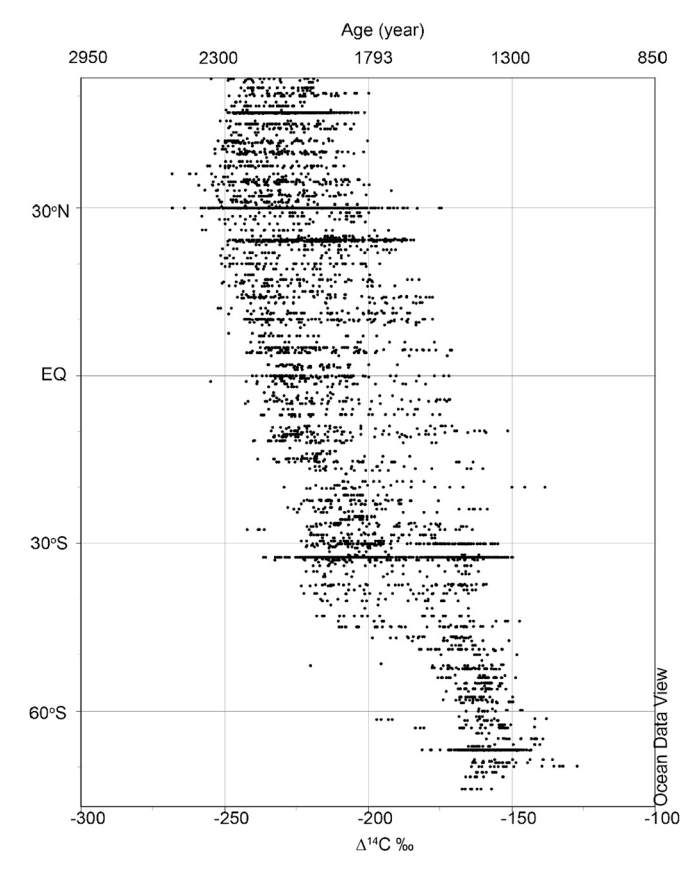


Fig. 8. Δ^{14} C and corresponding age of DIC from deep waters (>1500 m) in the Pacific vs. latitude. All data are from the GLODAP 2 database (Key et al., 2015).

radiocarbon, and the loss of oxygen via respiration (Fig. 9). For a 100% decrease in Δ^{14} C, oxygen decreases by about 100umol/kg. This relationship between abyssal water mass aging and dissolved oxygen depletion places an important limit on how "old" these abyssal waters can become before they would be devoid of dissolved oxygen and lose the capacity to support aerobic organisms that inhabit the sea floor. Extrapolating from the relationship shown in Fig. 9, if the residence time of abyssal waters were to increase by 1000 years, the deep Pacific would be anaerobic. This does not occur in the modern ocean because the rate of overturning is sufficient to replenish the bottom waters with oxygenated waters from the Southern Ocean. But if in the glacial ocean the rate of overturn was slower it is possible that the oceans consumed more oxygen and in doing so accumulated additional respired CO_2 , which would lower atmospheric CO_2 concentrations.

Stott (2023) examined the distribution of ventilation age estimates from the Rafter et al. compilation, focusing on the Pacific below 2500 m and between 20°S and 65°N. The Pacific being the largest carbon reservoir and the basin with the oldest and most oxygen depleted deep water, would be most sensitive to a decrease in ventilation rate during and ice age. The ¹⁴C database contains ventilation age estimates for both the Holocene and the LGM (Fig. 10A). It is clear from looking at the entire dataset from the deep Pacific that there are clear age biases in cores from low sedimentation rate environments, most likely due to bioturbation. Cores with sedimentation rates of <15 cm/ky exhibit a wide dispersion of ages for both the Holocene and LGM (Fig. 10A). Breaking out the LGM samples (Fig. 10B) the average ventilation age for cores with sedimentation rates between 1 and 5 cm/ky is 3162 years (median = 2871 std. = 376). Cores with sedimentation rates of 5-10 cm/ ky have average ventilation age of 3164 years (median = 3108 years, std. =655 year). Cores with sedimentation rates of 10-20 cm/ky the average is 2705 years (median 2627 years, std. =779 years). But cores with sedimentation rates above 20 cm/ky have an average ventilation

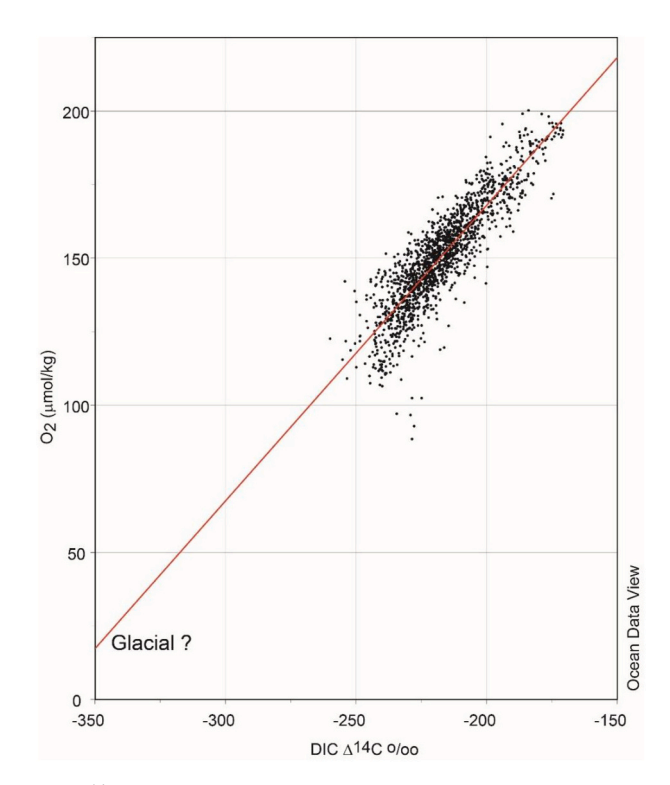
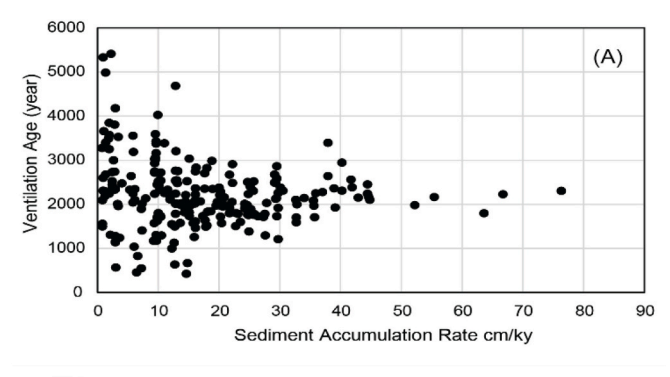


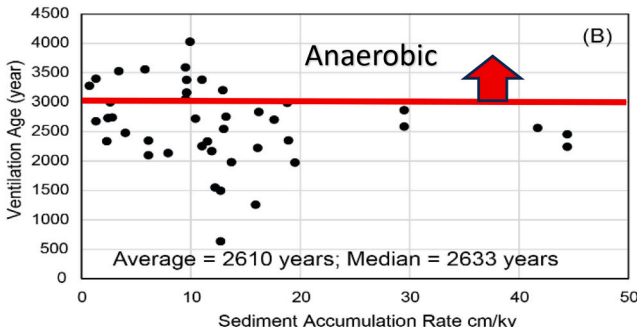
Fig. 9. Δ^{14} C of DIC from abyssal depths in the North Pacific (see map inset from Fig. 1) vs. dissolved oxygen from the same suite of samples. The red line is least squares fit. If abyssal ages were to increase by a thousand years above modern, it would imply a loss of ~ 100 um of O_2 which would have made the abyssal Pacific anaerobic. (For interpretation of the references to colour in this figure legend, the reader is referred to the web version of this article.)

age of 2449 years (median = 2627 years, std. =779 years). These higher sedimentation rate records are much closer to modern values.

The second consideration is the implication of ventilation age estimates older than 3000 years. If these ventilation age estimates were correct it would imply that the abyssal Pacific was anaerobic during the glacial, which was not the case. Hence, filtering the data for records that are <3000 years and using cores with sedimentation rates above 5 cm/ ky gives an average ventilation age for the glacial abyssal Pacific of 2179 years (Fig. 10C), which is indistinguishable from modern ventilation ages in the deep Pacific. We therefore find that the ocean-only hypothesis fails this test. We find no evidence among the cores with high fidelity that the ventilation rate was slower during the LGM. But this assessment disagrees with a recent paper by Skinner et al. (2023). These authors make a case that regional patterns of surface-deep (planktic-benthic) ¹⁴C age contrasts (used as metric of ventilation rate) can still be used, even with cores with very low sediment accumulation rates and widely varying ventilation ages. Using the available ¹⁴C database, they argue ventilation rates decreased in the deep Pacific by >800 years during the LGM. If true, the deep Pacific would have been virtually anoxic, which was not the case.

Where do things stand on this important scientific question? Clearly, there is too few ^{14}C data from high deposition rate environments, particularly in the Pacific. But when we put the results of our analysis of ^{14}C ventilation ages together with the analysis of the $\Delta\delta^{13}\text{C}$ data presented in the previous section, both metrics are at odds with the notion that the deep ocean sequestered excess respired carbon in a more slowly circulating ocean during the last glacial maximum.





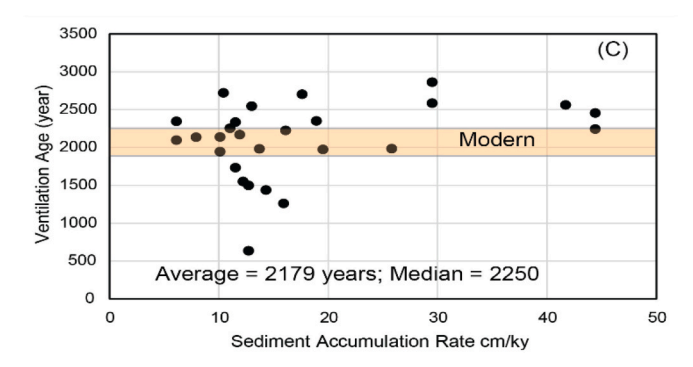


Fig. 10. Panel A is the entire 14 C ventilation age dataset from the Pacific sites below 2500 m (Rafter et al., 2022).

Panel B contains all LGM ventilation age estimates below 2500 m. Note that ages older than 3000 years would be anaerobic.

Panel C has been filtered to exclude ventilation age estimates >3000 years and cores with sedimentation rates below 5 cm/ky.

The shaded region is the range of modern ventilation ages in the deep Pacific.

2.5. Prediction 3: The $\Delta^{14}C$ and $\delta^{13}C$ gradients between the surface ocean and deep ocean would decrease during a glacial termination if the ocean-only model is correct

For the same reasons that the ocean-only model predicts increased vertical gradients in $\Delta^{14} C$ and $\delta^{13} C$ during a glaciation it also predicts a decrease in these gradients during a deglaciation as atmospheric CO2 was rising because old, respired CO₂ would be ventilated from the deep sea and replaced by younger waters with higher Δ^{14} C and δ^{13} C. Testing these predictions with existing records is challenging because to assess whether these isotope gradients were decreasing as CO2 began to rise requires records with sufficient temporal resolution and accurate age models. For example, during the last glacial retreat atmospheric CO2 rose by approximately 40 ppm within 4ky between 18.5 and 14.5kyBP. There are few marine isotope records that can resolve changes in the surface to deep water isotope gradients with sufficient resolution to assess whether this prediction is valid. There are, however, several cores from the Pacific that do have sufficient temporal resolution and enough benthic and planktic $^{14}\mathrm{C}$ age measurements that extend through the deglaciation. Taking advantage of these higher resolution rate cores

Stott et al. (2021) found no decrease in the surface to deep Pacific $\Delta^{14}C$ gradient during the early deglaciation (Fig. 11) as the ocean-only model predicts. The $\Delta^{14}C$ values decreased by approximately 100% during the Heinrich 1 interval in parallel with the upper ocean and atmosphere whereas the ocean-only model predicts a 100% increase in $\Delta^{14}C$ during the early deglaciation (Fig. 11). The surface-deep $\Delta^{14}C$ gradient remained constant throughout the rest of the deglaciation.

Two of the cores used in the Δ^{14} C assessment also have well-resolved benthic δ^{13} C records across the early deglaciation, including the H1 interval (Fig. 12). Neither of the cores document a rapid increase in δ^{13} C during the H1 interval that would be expected from an increased ventilation rate of the deep Pacific and the ventilation of excess respired metabolic carbon. The values from the early deglacial are the same as those from the LGM (Fig. 12). The benthic values do not begin to increase until after 14kyBP. The ocean-only hypothesis fails these tests as well.

2.6. Prediction 3: Calcite preservation increased in the deep Pacific during the early deglaciation as respired carbon is ventilated to the atmosphere

Carbonate cyclicity during the Pleistocene has been studied for decades (Arrhenius, 1952; Berger, 1977; Berger, 1982; Broecker, 1971). But most early studies lacked sufficient temporal resolution and age model constraints to elucidate the precise timing of carbonate changes.

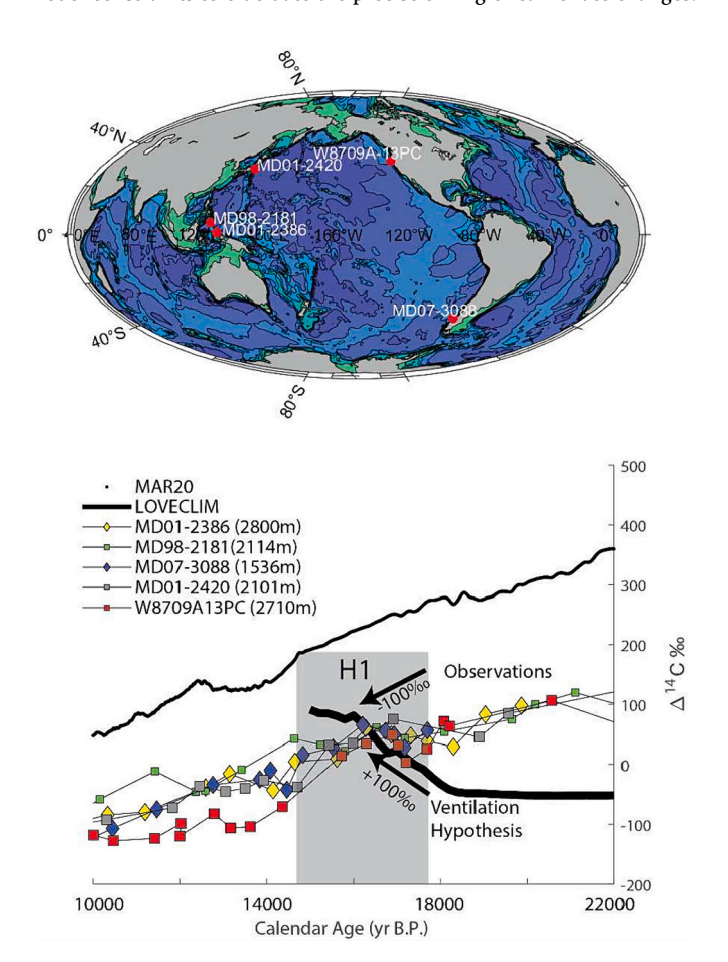


Fig. 11. From Stott et al. (2021). Upper panel deep Pacific core locations. Lower panel benthic $\Delta^{14} C$ from the deep Pacific cores. Lower Panel, MARINE20 (global surface ocean) $\Delta^{14} C$ (Heaton et al., 2020). The solid black line is the simulated deep Pacific (130 E–130° W, 0–50° N, and 2000–3000 m) $\Delta^{14} C$ response to enhanced ventilation during the deglaciation using the LOVCLIM model (Menviel et al., 2018). The $^{14} C$ ages from Core MD01–2386 (Broecker et al., 2008), MD07–3088 (Siani et al., 2013); MD01–2420 (Okazaki et al., 2012), MD98–2181 (Stott et al., 2021) and W8709A-13PC (Lund, 2013).

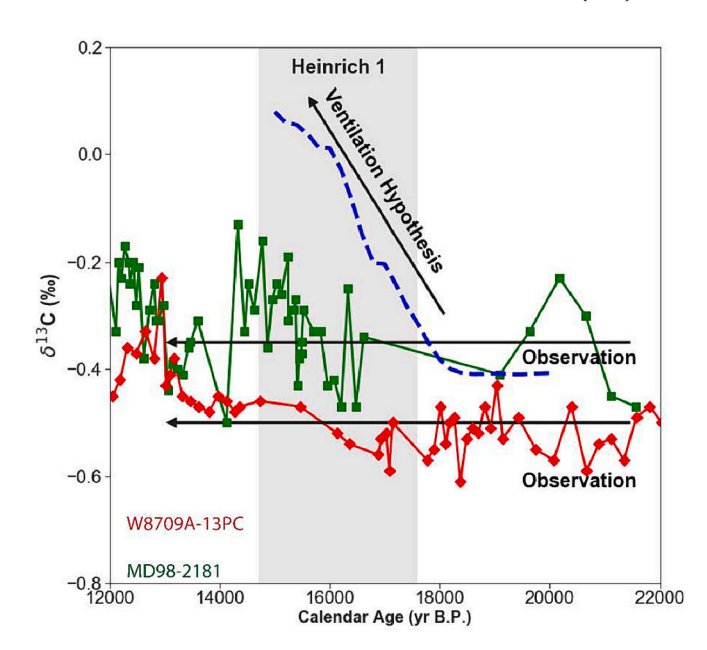


Fig. 12. *Cibicidoides* δ^{13} C from deep Pacific cores MD98–2181 (green) (Stott et al., 2021), W8709A-13PC (red) (Lund and Mix, 1998; Lund et al., 2011), and the LOVECLIM model simulated Deep Pacific δ^{13} C_{DIC} (blue dashed line) response to enhanced ventilation (Menviel et al., 2018). (For interpretation of the references to colour in this figure legend, the reader is referred to the web version of this article.)

That limitation has been rectified to a large degree with better age model constraints and higher resolution records from each of the ocean basins (Anderson et al., 2008; Farrell and Prell, 1989; Mekik et al., 2012; Sexton and Barker, 2012). It is now clear that the Pacific and Atlantic basins experienced opposite changes during glacial/interglacial cycles during the late Pleistocene. The deep Pacific saw increased calcite preservation during glacials whereas the Atlantic experienced reduced preservation. In the deep Pacific for example, Farrell and Prell showed that the calcite lysocline deepened by several hundred meters during late Pleistocene glacials and shoaled during interglacials. This seems counterintuitive to the notion that the deep ocean stored excess respired carbon during glaciations and can only be reconciled if there was a net increase in alkalinity in the deep Pacific during glaciations. We have no direct way to measure of paleoAlkalinity but there are proxies for $[CO_3^{\pm}]$ (Doss and Marchitto, 2013; Yu et al., 2010; Yu et al., 2013). B/Ca estimates of [CO₃⁼] for the LGM are similar to modern (Fig. 13). These records also document higher B/Ca values in the post glacial sections of the cores. The highest values occur during between 15 and 10kyBP (Fig. 13). These records have been interpreted to reflect a decrease in



Fig. 13. B/Ca-based estimates of $[CO_3^-]$ from benthic foraminifera taken from cores in the western equatorial Pacific (Yu et al., 2010).

deep Pacific DIC during the deglaciation in response to ventilation of excess respired carbon. But it is important to note that there was no change in $[CO_3^-]$ at 2.3 km during the deglaciation (Fig. 13), which is also the case in the eastern equatorial Pacific (Doss and Marchitto, 2013). This too is counterintuitive because if the deep Pacific ventilated excess respired carbon during the deglaciation from the abyssal Pacific that carbon would have passed through the intermediate depth Pacific on its return to the Southern Ocean and thus, there should be evidence of lower $[CO_3^-]$ at intermediate depths during the deglaciation. This is not evident in the B/Ca records (Fig. 13). An alternative interpretation of the increased $[CO_3^-]$ values 15kyBP as seen in the B/Ca results from abyssal depths would be increased calcite dissolution and shoaling of the lysocline as documented by Farrell and Prell (1989). In other words, the higher $[CO_3^-]$ in the abyssal Pacific would reflect higher alkalinity rather than a decrease in the DIC.

There have been efforts to look for an increase in carbonate preservation during the early deglaciation that would accompany enhanced ventilation of excess DIC and increased $[CO_3^-]$ as predicted by the prevailing hypothesis. But these efforts have failed to find a calcite preservation event in the early deglaciation in the Pacific, or in the Atlantic or Indian Oceans (Mekik et al., 2012). So, taken together these data fail to validate the prevailing hypothesis.

2.7. Prediction 4: Ice minima align with maxima in solar radiation at high northern latitudes

The orbital theory predicts that ice minima should correspond with

summer season maxima at high northern latitudes (Ates, 2022). Over the past 2.5 million years Earth's climate spent most of the time becoming colder and more glaciated and a small percentage of time becoming warm and staying warm (Fig. 14). This temporal asymmetry is another challenge to the orbital theory of ice ages. For example, Köhler and van de Wal (2020) pointed out that the minima in land ice extent were not well correlated with maxima in obliquity as Milankovitch theory predicts. In fact, during the late Pleistocene ice sheet minima coincided with obliquity maxima only 52% of the time (Fig. 2). Hobart et al. (2023) provides a summary of hypotheses that have attempted to reconcile why the timing of glacial-to-interglacial transitions have not aligned with obliquity maxima as the original orbital theory predicts. Their work leverages newly updated age models for marine $\delta^{18}\!O$ records, to suggest that Pleistocene glacial "terminations" occurred when precession was approaching a maxima in association with higher obliquity. However, an inspection of these records reveals that this orbital configuration with increasing precession and obliquity also occurred during glaciations as the climate was becoming colder, not just when an ice sheets were retreating (yellow lines in Fig. 14). It seems inescapable that orbital forcing alone is not enough to explain the timing of glacial/interglacial transitions nor why southern hemisphere glaciers retreated simultaneously with those in the northern hemisphere. Combined with the fact that interglacials have been short-lived suggests that the climate system has tried to remain glaciated, but interruptions occurred when atmospheric CO2 rose and changed the negative radiative balance. For this reason, it is crucial to learn what regulated the release of CO2 to the atmosphere at during periods of warming and ice retreat.

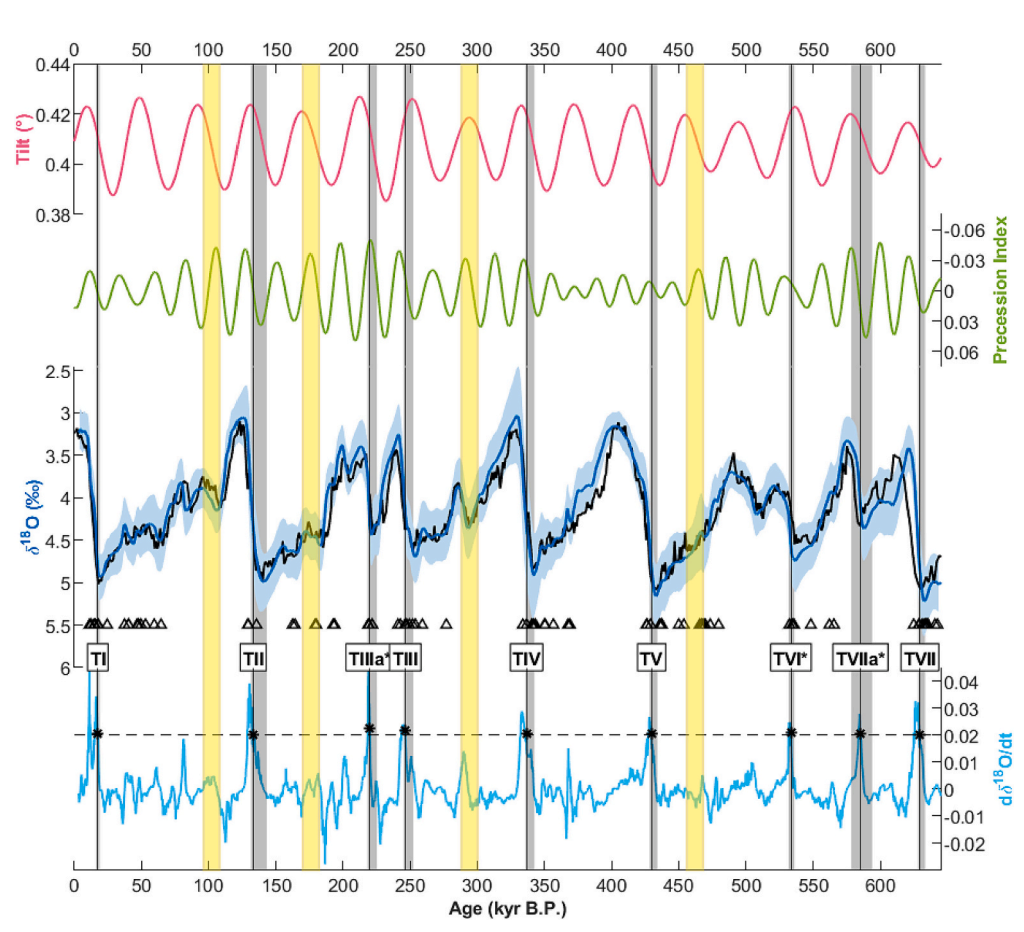


Fig. 14. Modified from Hobart et al. (2023). The bottom panel is the derivative of the δ^{18} O record as a function of time. Note the high percentage of time δ^{18} O was negative or decreasing. The grey vertical bars in the upper panel are intervals identified in the original study as times of glacial/interglacial transition when precession and obliquity are approaching their combined maxima. The yellow vertical bars (added here) are intervals when both precession and obliquity were aligned at their maxima, but the climate was becoming colder, and ice sheets were advancing. (For interpretation of the references to colour in this figure legend, the reader is referred to the web version of this article.)

3. Is the inventory of carbon in the reactive zone fixed?

3.1. Geologic carbon fluxes to the reactive zone

Four decades ago, the number of records available to evaluate the validity of the Milankovitch theory was small. Yet, those early findings still hold today. There is a natural rhythmicity to Earth's climate variability and that rhythmicity has been replicated over and over in data from both terrestrial and marine archives. The frequency of variability is similar to Earth's orbital cycles. But two facts require a re-consideration of the way the orbital theory of climate is thought to operate. The first is that there has not been a consistent relationship between the timing of ice minima and the maxima in solar forcing (Fig. 2). Nor has there been a consistent relationship between the timing of glacial to interglacial transition and orbital phasing (Fig. 14).

The second fact is that orbital variations cannot explain the synchroneity in ice advance and retreat in both hemispheres. Greenhouse gases are necessary to explain both the timing and magnitude of warming that brings about ice retreat in both hemispheres because it accounts for nearly 50% of the radiative forcing change. So, why does atmospheric CO2 vary with ice volume? In the previous section we looked for evidence that would support the notion that there is a feedback between the orbital scale climate variability and the ocean's response to that variability by affecting biological uptake and deep ocean carbon storage during a glacial state and release of that carbon at a critical point in the orbital cycle. We found that the data fail to validate this ocean-only hypothesis, and the associated assumption that the size of the reactive pool of carbon remains constant. Broecker et al. (2015) came to this same realization. Having been at the frontier of the Milankovitch revolution in the 1960s and having had a significant influence on the convention that the oceans are a grand climate capacitor, he concluded that something was missing and pointed to the potential role of geologic processes that could influence the inventory of carbon in the reactive zone.

Huybers and Langmuir (2009, 2017) have worked on an alternative to the prevailing ocean-only model. They've explored how geologic carbon fluxes could vary on glacial interglacial timescales in response to the growth and retreat of ice sheets and sea level change, which affects hydrostatic pressure over the mantle and in doing so influences the rate of magma flow to the Earth's surface via terrestrial and submarine volcanic sources. The model employed is a simple one, which lacks many of the dynamics in the Earth System. Yet, it points to a potential way for there to be a non-steady state flux of carbon to the ocean-atmosphere on glacial time scales. And in this sense the inventory of carbon would not be constant as the prevailing hypothesis asserts. One of the challenges to this model is establishing the timing between ice sheet growth and the flow rate of carbon from the mantle, a subject of ongoing experimentation and evaluation (Connolly et al., 2009). In the Huyber and Langmuir model the time scale of carbon migration to the crust from the mantle is a model parameter that can be varied to affect the timescale of CO_2 release. Setting this delay parameter to ~ 10 ky simulates a ~ 120 ky response time for buildup of ice on land and sea level fall to promote a release of carbon at mid ocean ridges. The link to orbital timescale is the length of time required to build sufficiently large ice sheets that lowers sea level enough to affect a decompression of the mantle and a migration delay timescale. Observational data needed to test this model is still very limited.

Lund and Asimow (2011; 2016) were able to show that hydrothermal metal fluxes increased in both the Atlantic and Pacific during MIS 2 and 4. Similar findings were made by Middleton et al. (2016). These observations are consistent with Huyber and Lanmuir's reasoning and consistent with the expectation that sea level affects decompression melting and enhanced magma flux. Interestingly these observational studies found that metal fluxes began to increase around 25kyBP and peaked during the deglaciation as atmospheric CO_2 was rising. How much additional CO_2 would be associated with enhanced magma and

metal flux is still uncertain (Cartigny et al., 2008). Nonetheless, while not proof that sea level effected magma fluxes enough to influence the carbon budget, the correspondence between the increased metal fluxes and sea level lowering are additional reasons to consider that the carbon budget need not be in balance on glacial/interglacial time scales.

During the same period these studies were taking place there were several discoveries from each of the ocean basins that documented large $^{14}\mathrm{C}$ age anomalies in marine carbonates deposited at the end of the last ice age. Marchitto et al. (2007) first documented a large -200% deglacial Δ^{14} C excursion from a shallow-intermediate depth core (705 m water depth) near Baja. The radiocarbon excursion persisted for about 4ky between 18 and 11kyBP. It was originally interpreted to reflect ventilation of an old deep-water mass that had been isolated in the deep sea during the glacial and then ventilated through Antarctic Intermediate Waters to the northeastern Pacific. Intrigued by the magnitude of the Baja excursion Stott et al. (2009) revisited a shallow-intermediate water depth core in the eastern equatorial Pacific, core VM21-30 (617 m water depth) from which Broecker et al. (2004) had previously found an anonymously 'old' 14C age at the same deglacial time interval as the Baja record of Marchitto et al. Broecker et al. considered the Galapagos ¹⁴C age erroneous and an artifact of disturbance. However, when Stott et al. resampled the core, they found that the ¹⁴C age excursion matched the timing seen in the Baja excursion. What's more, there was no excursion in the planktic foraminifer ¹⁴C ages in the same samples. The excursion was only in the benthic values. There was no indication in the benthic δ^{18} O record of a disruption in the stratigraphy. The magnitude of the excursion in the VM21-30 core was much larger than the one found near Baja. In fact, the age anomaly in the benthic records was as much as 8000 years. There is no way this excursion could reflect the ventilation age of an old water mass as Marchitto et al. originally envisioned. Waters that old would have been anoxic and therefore unable to support an aerobic benthic community.

Bryan et al. (2010) then documented additional shallow-water deglacial radiocarbon age anomalies in cores from the Arabian Sea. Here too the excursions are very large, on the order of -200 to -300%. Again, the authors attributed these shallow water excursions to the ventilation of old waters from the deep sea (Lindsay et al., 2016). Since those earlier studies were published, more deglacial ¹⁴C excursions have been documented in other parts of the global ocean. Stott and Timmermann (2011) replicated the VM21-30 results in another core on the Galapagos margin, VM21-19 and showed that the magnitude of the excursion at this site was also too large to be explained by ventilation of an old water mass. Rafter et al. (2019) documented large ¹⁴C anomalies in the Gulf of California similar in timing and magnitude those found off Baja by Marchitto. But the Gulf of California excursion appears to have begun earlier, during the late glacial. Stott et al. (2019b) then examined the geochemistry and carbonate preservation across the deglacial excursions in the Galapagos cores finding carbonate preservation dropped dramatically during the excursion and was associated with increased accumulation of hydrothermal metals. The authors proposed that the radiocarbon excursions were produced when hydrothermal fluids were released during the deglaciation from nearby geologic sources (Stott and Timmermann, 2011; Stott et al., 2019b). They further suggested that given the shallow-water location in the zone of equatorial upwelling, it was likely that the CO2 rich waters exchanged carbon with surface waters and those surface waters would have ventilated old carbon to the atmosphere, thereby affecting the ocean-atmospheric carbon budget.

Radiocarbon anomalies during the last deglaciation have now been documented at multiple sites from each ocean basin (Fig. 15). There are likely more locations in the ocean where ¹⁴C anomalies of this kind formed at the last glacial transition. But there are still only a few shallow-intermediate water depth cores that have been investigated. And not all ¹⁴C age anomalies occurred at shallow water depths. There are also large deglacial ¹⁴C excursions at deeper water sites (Ronge et al., 2019; Ronge et al., 2016; Sikes et al., 2000). These sites are not near hydrothermal vents. The large ¹⁴C age anomalies from both shallow and

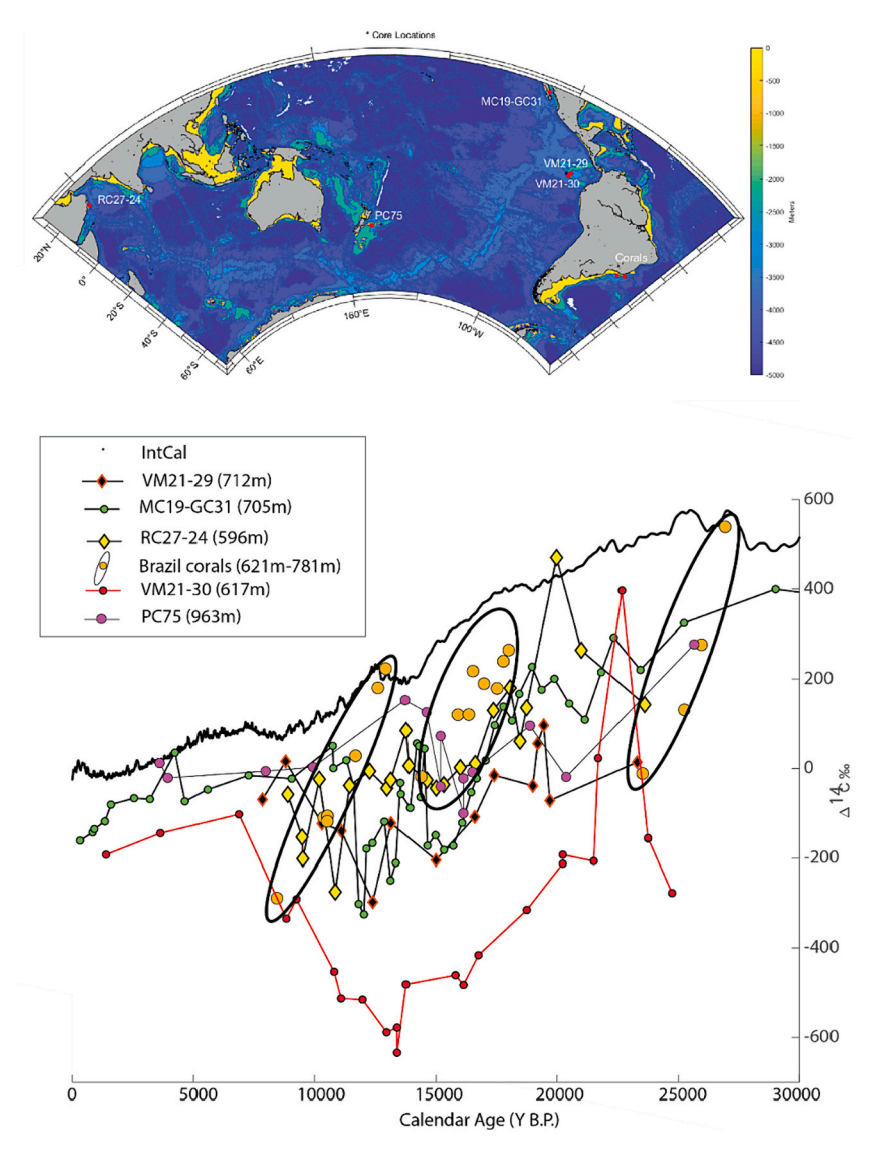


Fig. 15. Shallow-intermediate depth sites where large negative deglacial Δ^{14} C anomalies have been found (Stott, 2020).

deep water sites in the southwest Pacific on the Chatham Rise are found in association with pockmarks (Stott et al., 2019a) that overlay subsurface conduits that act as pathways for carbon rich fluids to migrate to the surface. There are thousands of pockmarks across the Chatham Rise. Establishing when these pockmarks formed is a challenge because only a few have been dated. Of those that have been studied, they formed at the end of the last glaciation (Stott et al., 2019a).

As more of these types of records become available it is increasingly evident that geologic carbon was leaking to the ocean at the end of the last ice age. While it is premature to estimate how much carbon leaked from these geologic sources, the magnitude, and the duration of the ¹⁴C excursions in each ocean suggests these were significant sources of additional carbon being added to the ocean and a further indication that the carbon budget was not in steady state. The suggestion that geologic carbon release could have influenced the global carbon budget and atmospheric CO₂ has been provocative. This was also the case when the PETM event was first described (Kennett and Stott, 1991). Most paleoceanographers are not familiar with research of geologic CO₂ stored in near surface reservoirs (Camilli et al., 2015; Chivas et al., 1987; German et al., 2022; Inagaki et al., 2006; Lupton et al., 2006; Lupton et al., 2008) or that hydrothermally derived carbon could vary significantly on glacial/interglacial timescales.

Shallow subsurface carbon reservoirs are not currently included in

the marine carbon budget. And it's not clear how these reservoirs could be incorporated into the ocean carbon budget since the fluxes are not known and may be highly variable. A characteristic of near surface carbon reservoirs are thin hydrate caps that limit carbon release (Fig. 16). When disturbed however, large quantities of carbon can be released rapidly (Inagaki et al., 2006). Nealson (2006) described the reservoir of liquid CO2 in the back arc basin of the Okinawa Trough as a "Lake of Liquid CO2". There is another "lake" of liquid CO2 at the bottom of the Aegean Sea (Camilli et al., 2015). An example of how much carbon can leak from these reservoirs was described by Lupton et al. (2006, 2008). These authors discovered active vents among the volcanic islands on the Mariana in the western Pacific. There are numerous vents in this region. One of them is a small vent, "Champagne", located in about 1600 m water depth. This vent was found to be discharging droplets of nearly pure liquid CO₂. The droplets were emanating from a reservoir just beneath the sediment surface that is capped by a hydrate (Fig. 16). By counting the rate at which bubbles of liquid CO2 were discharging they estimated a carbon flux from this small hole on the seafloor of 23 mol CO_2/s , which amounts to about 0.1% of the estimated global mid ocean ridge flux. When the surface was disturbed, the rate increased significantly. It is also worth noting that the δ^{13} C of liquid CO₂ from this site is -1.8 to -1.2% (Lupton et al., 2008), close to (albeit slightly more negative) than deep water DIC but much higher than respired metabolic

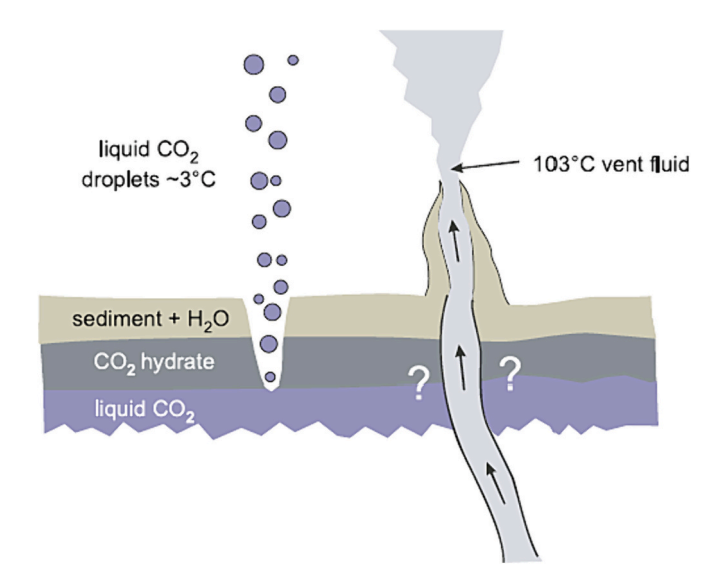


Fig. 16. From Lupton et al. (2008) depicting the environment at the Champagne vent site where liquid $\rm CO_2$ accumulates beneath a hydrate cap. The total amount of $\rm CO_2$ residing in the subsurface is not known but the estimated flux from this single hole is about 0.1% of the global mid ocean ridge flux.

CO₂. The high δ^{13} C values are attributed to the origin of the liquid carbon, which is surmised to originate from subducted marine carbonates. The same is likely the case at sites in the southwest Pacific where large 14 C anomalies are found without correspondingly large δ^{13} C anomalies (Stott et al., 2019a). These examples and observations make the point that there are potentially many locations in the oceans where geologic CO₂ accumulates in large quantities and can leak into the ocean if disturbed. Hydrate caps are sensitive to both temperature and pressure, making them potentially sensitive to changes in sea level that accompanied glaciations.

3.2. The rapid and transient variations in atmospheric CO_2 during each glaciation?

During late Pleistocene glaciations (Fig. 1) there were rapid declines in atmospheric CO_2 following each transition. In fact, there were multiple excursions in atmospheric CO_2 throughout each glaciation. For example, there was a \sim 35 ppm drop in atmospheric CO_2 between 115-108kyBP during the MIS 5–4 transition. These rapid declines were followed by similarly rapid increases in atmospheric CO_2 , although the increases were not as large as the declines that preceded them. Consequently, the overall trend is a long-term decline in atmospheric CO_2 that culminated in average glacial minima of about 180 ppm (Fig. 1). It is this long-term decline that is the focus of this paper. The short-term variations pose a challenge to explain.

It would seem at first that the rates of drop during the rapid variations could not be explained solely from removal/release of carbon from the reactive zone because the time scales are so short. It would seem more likely that these transient variations were part of the ocean/atmospheric dynamic that was undergoing change throughout a glaciation. In a recent paper by Garity and Lund (2024) the authors found that there was an increase in the shallow-intermediate to deep water $\delta^{13}C$ gradient in the southwest Atlantic during the MIS5-4 transition. This was temporary, however. The deep water benthic δ^{13} C values increased again during MIS 3 and the shallow-deep water gradient was restored. The authors make a case that these transient variations reflect shoaling of the deep/intermediate water boundary, which would imply a greater proportion of southern sourced waters in the deep Atlantic during these transitory intervals. The magnitude of change reflected in the $\delta^{13}C$ gradient change would suggest the deep Atlantic was temporarily storing additional carbon during these excursions and that could have contributed to the rapid drop in atmospheric CO₂.

Given the focus of the present study on the potential imbalance of sources and sinks of carbon we were prompted to look at sea level reconstructions (Rohling et al., 2009) and consider their potential implications. The sea level reconstructions depict rapid drops that were closely aligned with the rapid declines in atmospheric CO2. For example, there is a 40m drop in sea level between 125 and 108kyBP (Fig. 17). The consequence of this would be an increase in the concentration of dissolved Ca in the ocean because the volume of the ocean decreased. Taking the modern CaO flux estimate of Lasaga et al. (1985), which Broecker and Sanyal (1998) used in their calculations to assess the carbonate compensation response to changes in the input/outputs of CO2 and CaO from weathering and converting the sea level fall at the MIS 5 transition to an estimate of ocean volume change of about 1%, would have increased the Ca concentration by 20umol/l in roughly 10ky. That would have produced a correspondingly change in carbonate compensation if it was not accompanied by a change in fluxes. This was followed by a rise in sea level that coincided with a rise in atmospheric CO₂. This happened repeatedly during the glaciation. At the LGM, the sea level induced change in ocean volume was about 3% (the value used by the PMIP group, Lhardy et al., 2021) and that would have caused an increase in Ca concentration of 60umol/lt compared to the modern ocean, assuming the transport of CaO by rivers did not change. This consideration is raised because the ocean's volume was varying. It was lower than the modern most of the time during the Pleistocene. Whereas Broecker and Sanyal (1998) estimate of the CaO flux for a steady state modern ocean is 2142umol/l/Myr (they use a value of 2000umol/l/ Myr) and ocean volume was held constant, the actual long-term flux spanning a million-year time scale would be better approximated by the glacial ocean volume. That would produce a flux value of 2165umol/l/ Myr or about 165umol/l higher than the value used by Broecker and Sanyal's calculations, and that assumes there was no change in river transport.

Lasaga et al's modern-day CaO flux used by Broecker and Sanyal was an estimate needed to make the BLAG model simulate a quasi-steadystate modern carbon system. This modern ocean estimate may not be a good representation of the glacial world that characterized most of the Pleistocene. Sea level variability itself does not change weathering rates. But sea level is coupled to climatic changes that can affect weathering fluxes. As one example, over the Pleistocene glacial advances eroded calcium rich terranes that once covered eastern Canada. By the late Pleistocene, much of that rock had been removed from eastern Canada exposing the underlying shield. Consequently, today lakes of western Canada are alkaline whereas the watersheds of eastern Canada are acidic. That observation alone implies a change in weathering regime from the early to late Pleistocene within this glaciated region. The takeaway should be that without clear evidence for excess carbon storage in the deep sea, seeking better knowledge of weathering rates and fluxes takes on great importance.

4. The Pleistocene glaciations in the context of Earth's long-term cooling during the Cenozoic

This contribution began with a question: Glacial Terminations or Glacial Interruptions? The premise being that perhaps the natural state of the climate system is a glaciated state, and short warm intervals (interglacials) are interruptions caused by transient episodes of $\rm CO_2$ release to the ocean/atm from geologic sources. The time between interruptions in this hypothesis is dictated by the process(s) that regulate how long it takes for the carbon cycle to recover from an interruption and return to a glaciated state. This would depend on how much $\rm CO_2$ must be removed from the ocean and atmosphere to bring the climate back to a cold glaciated condition. The processes involved in the removal would include enhanced carbon burial both in the ocean and in the terrestrial biosphere.

During the late Pleistocene the overall compensation period was

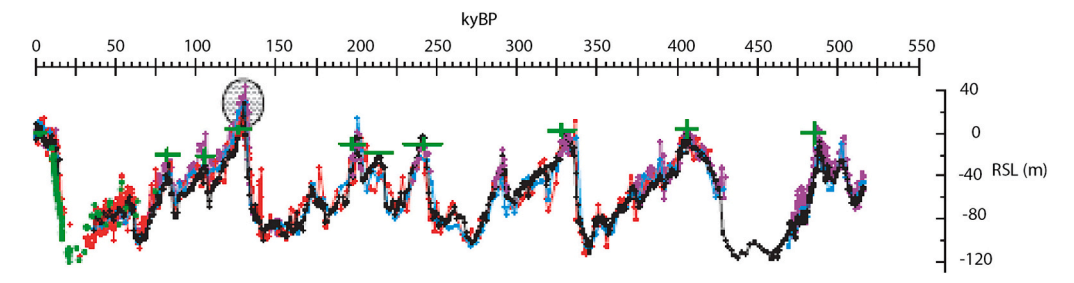


Fig. 17. Reconstructed relative sea level from Rohling et al. (2009) spanning the late Pleistocene. The shaded circle marks the onset of the last glacial and the rapid sea level fall during MIS 5.

100ky, which may have been punctuated by variations (as described in the previous section). The amount of $\rm CO_2$ removed over a glaciation is reflected in the \sim 80-100 pm change observed in the ice core records. The removal process need not be fundamentally different from the modern but could have been larger (see previous section). The most recent interruption for which there are data began around 25kyBP and peaked during deglaciation (Bryan et al., 2010; Lund and Asimow, 2011; Lund et al., 2016; Marchitto et al., 2007; Middleton et al., 2016; Rafter et al., 2019; Ronge et al., 2016; Stott et al., 2019a; Stott et al., 2019b).

Stepping back in time and viewing the Pleistocene glaciations from the perspective of the past 50 million years, one can view the last 2.5 million years of cooling and increasing glaciation as a continuation of a longer-term cooling trend that began in the Eocene (Fig. 18). In fact, if one were to change the timescale on the lower axis of Fig. 18 and adjust the scale of the Y axis, the Cenozoic record looks very much like a glacial cycle of the late Pleistocene. The Earth's climate has been in a long-term glacial cycle for millions of years. This long-term cycle is attributable to the same reasoning proposed here, the removal of carbon from the reactive zone via carbon sequestration outpaced release of carbon from geologic sources (Berner et al., 1983; DeConto and Pollard, 2003; Li and Elderfield, 2013; Raymo and Ruddiman, 1992; Wallmann, 2001).

5. Summary and path forward

After a century of scientific pursuit there have been major advances in documenting the timing, magnitude, and recurrence of large climatic changes spanning Earth's past 60 million years. There is a well-documented rhythm of climate variability during the past 2.5 million

years that shares frequencies like Earth's orbital cycles. This realization was a major accomplishment in the mid-20th century. The acquisition of records of greenhouse gas variability was another major scientific advance later in the 20th century. Yet, we still lack a satisfactory theory to explain how Earth's climate system operates in response to the small changes in solar forcing that accompanied eccentricity, obliquity, and precession variability. The original theory does not explicitly predict how orbital variations lead to systematic changes in the concentration of atmospheric CO_2 . So the challenge is to understand all the processes involved, including geologic processes. That includes an accurate depiction of each variable involved in the carbon cycle that affects the rhythmic nature of atmospheric CO_2 variability.

A case has been made here that the ocean-only model has a fundamental flaw. It excludes geologic processes by assuming they operate too slowly to affect the carbon cycle on time scales of Pleistocene glaciations. It assumes that the carbon inventory of the reactive zone does not change on glacial/interglacial timescales. The initial elements of an alternative hypothesis set forth here predict that the carbon cycle is not in balance and carbon input fluxes are outpaced by carbon output fluxes except when there are interruptions. We cannot reject this hypothesis. But the data to test this hypothesis is limited. We need better estimates of how geologic carbon fluxes changed in response to compression/ decompression of the mantle as ice advanced and retreated. This is a critical variable in the carbon budget. Similarly, it's important to expand on the small database of records that provide fingerprints of geologic processes, like the radiocarbon anomalies and metal fluxes and what controls their timing and magnitudes. There is also work to be done to better constrain alkalinity fluxes across glacial cycles, which may vary

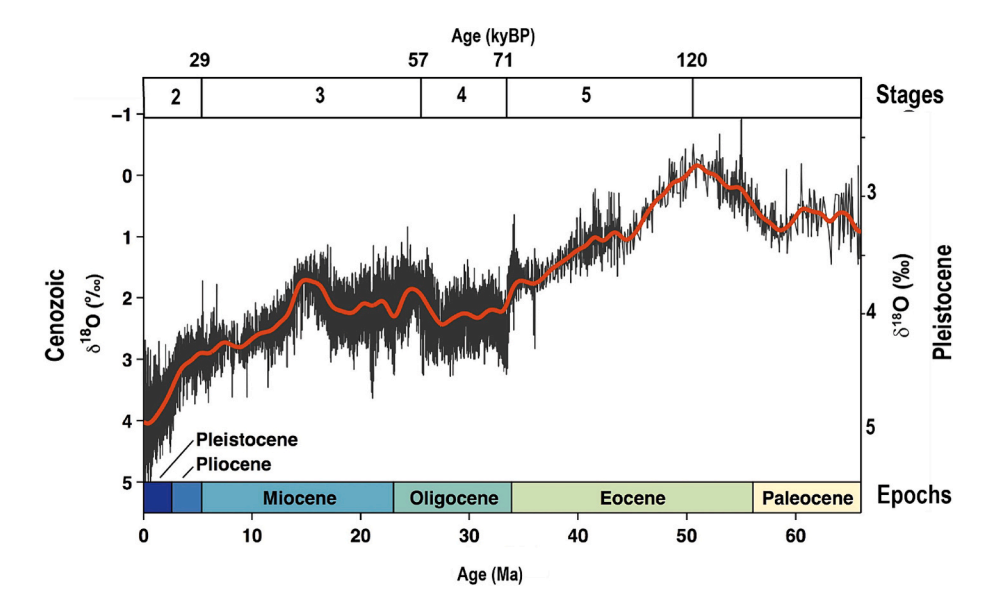


Fig. 18. The oxygen isotope compilation for the Cenozoic as depicted in Zachos et al. (2001). The figure has been modified to illustrate the similarity between a late Pleistocene glacial cycle (right-hand axis) and the associated marine isotope stages (upper x-axis) and the longer-term history of the Cenozoic glacial cycle.

significantly in response to glacial erosion and changing river runoff. And this alternative hypothesis would predict that if excess carbon from geologic sources contributed to the rise in atmospheric CO_2 at a glacial interruption, there should associated with carbonate dissolution. Carbonate dissolution is observed at the last glacial/interglacial transition in association with the large $\Delta^{14}\text{C}$ anomalies in the EEP. Additional data like this is needed to evaluate whether there is dissolution at other locations and at other glacial/interglacial transitions.

The acquisition of new observations and the development of new tools that accelerated in recent years is costly. Sea-going expeditions are expensive and there is great competition for available resources. For this reason, the paleoclimate community must work together to argue for the importance of obtaining new data while embracing new ideas that can lead to breakthroughs.

Declaration of competing interest

Lowell Stott reports financial support was provided by National Science Foundation. Lowell Stott reports financial support was provided by University of Southern California. If there are other authors, they declare that they have no known competing financial interests or personal relationships that could have appeared to influence the work reported in this paper.

Data availability

All data has been published previously

Acknowledgements

The author extends special appreciation to Stella Baldwin and Roman Ferraro for their help in collecting the $\delta^{13}C$ data and preparing the tables in this paper. Discussions with numerous colleagues has provided constructive advice and motivations. Thanks is extended to the authors whose figures have been used in this contribution. Special appreciation is extended to a reviewer who provided important questions. Funding for this work was provided by a grant to Stott from the National Science Foundation (OCE MG&G 1904433 and 1558990).

Appendix A. Supplementary data

Supplementary data to this article can be found online at https://doi.org/10.1016/j.earscirev.2024.104756.

References

- Anderson, R.F., Fleisher, M.Q., Lao, Y., Winckler, G., 2008. Modern CaCO3 preservation in equatorial Pacific sediments in the context of late-Pleistocene glacial cycles. Mar. Chem. 111 (1), 30–46.
- Anderson, R.F., Ali, S., Bradtmiller, L.I., Nielsen, S.H.H., Fleisher, M.Q., Anderson, B.E., Burckle, L.H., 2009. Wind-driven upwelling in the Southern Ocean and the deglacial rise in atmospheric CO₂. Science 323 (5920), 1443–1448.
- Anderson, R.F., Sachs, J.P., Fleisher, M.Q., Allen, K.A., Yu, J., Koutavas, A., Jaccard, S.L., 2019. Deep-sea oxygen depletion and ocean carbon sequestration during the last ice age. Global Biogeochem. Cycles 33 (3), 301–317.
- Archer, D., 2010. The Global Carbon Cycle. Princeton University Press.
- Arrhenius, G., 1952. Rate of production, dissolution and accumulation of biogenic solids in the ocean. Glob Planet Change 5, 1–128.
- Ates, M.E., 2022. Pioneers of the ice age models: a brief history from Agassiz to Milankovitch. Hist. Geo Space. Sci. 13 (1), 23–37.
- Barker, S., Knorr, G., 2021. Millennial scale feedbacks determine the shape and rapidity of glacial termination. Nat. Commun. 12 (1), 2273.
- Berger, W.H., 1977. Deep-sea carbonate and the deglaciation preservation spike in pteropods and foraminifera. Nature 269 (5626), 301–304.
- Berger, W.H., 1982. Increase of carbon dioxide in the atmosphere during deglaciation: the coral reef hypothesis. Naturwissenschaften 69 (2), 87–88.
- Berner, R.A., Caldeira, K., 1997. The need for mass balance and feedback in the geochemical carbon cycle. Geology 25 (10), 955–956.
- Berner, R.A., Lasaga, A.C., Garrels, R.M., 1983. The carbonate-silicate geochemical cycle and its effect on atmospheric carbon dioxide over the past 100 million years. Am. J. Sci. 283 (7), 641–683.

- Broecker, W.S., 1966. Absolute Dating and the Astronomical Theory of Glaciation. Science 151 (3708), 299–304.
- Broecker, W., 1971. Calcite accumulation rates and glacial to interglacial changes in ocean mixing. In: The Late Cenozoic Ice Ages, pp. 239–265.
- Broecker, W.S., Sanyal, A., 1998. Does atmospheric CO2 police the rate of chemical weathering? Global Biogeochem. Cycles 12 (3), 403–408.
- Broecker, W., Barker, S., Clark, E., Hajdas, I., Bonani, G., Stott, L., 2004. Ventilation of the Glacial Deep Pacific Ocean. Science 306, 1169–1172.
- Broecker, W., Clark, E., Barker, S., 2008. Near constancy of the Pacific Ocean surface to mid-depth radiocarbon-age difference over the last 20 kyr. Earth Planet. Sci. Lett. 274 (3–4), 322–326.
- Broecker, W.S., Yu, J., Putnam, A.E., 2015. Two contributors to the glacial CO₂ decline. Earth Planet. Sci. Lett. 429, 191–196.
- Bryan, S.P., Marchitto, T.M., Lehman, S.J., 2010. The release of ¹⁴C-depleted carbon from the deep ocean during the last deglaciation: evidence from the Arabian Sea. Earth Planet. Sci. Lett. 298 (1–2), 244–254.
- Burke, A., Robinson, L.F., 2011. The Southern Ocean's Role in Carbon Exchange during the Last Deglaciation. Science.
- Camilli, R., Nomikou, P., Escartín, J., Ridao, P., Mallios, A., Kilias, S.P., Argyraki, A., 2015. The Kallisti Limnes, carbon dioxide-accumulating subsea pools. Sci. Rep. 5, 12152.
- Cartapanis, O., Galbraith, E.D., Bianchi, D., Jaccard, S.L., 2018. Carbon burial in deepsea sediment and implications for oceanic inventories of carbon and alkalinity over the last glacial cycle. Clim. Past 14 (11), 1819–1850.
- Cartigny, P., Pineau, F., Aubaud, C., Javoy, M., 2008. Towards a consistent mantle carbon flux estimate: Insights from volatile systematics (H₂O/Ce, δD, CO₂/Nb) in the North Atlantic mantle (14° N and 34° N). Earth Planet. Sci. Lett. 265 (3), 672–685.
- Chen, H., Haumann, F.A., Talley, L.D., Johnson, K.S., Sarmiento, J.L., 2022. The Deep Ocean's Carbon Exhaust. Global Biogeochem. Cycles 36 (7) e2021GB007156.
- Chivas, A.R., Barnes, I., Evans, W.C., Lupton, J.E., Stone, J.O., 1987. Liquid carbon dioxide of magmatic origin and its role in volcanic eruptions. Nature 326 (6113), 587–589.
- Clark, P.U., Dyke, A.S., Shakun, J.D., Carlson, A.E., Clark, J., Wohlfarth, B., Mitrovica, J. X., Hostetler, S.W., McCabe, A.M., 2009. The last Glacial Maximum. Science 325 (5941), 710–714.
- Connolly, J.A.D., Schmidt, M.W., Solferino, G., Bagdassarov, N., 2009. Permeability of asthenospheric mantle and melt extraction rates at mid-ocean ridges. Nature 462 (7270), 209–212.
- DeConto, R.M., Pollard, D., 2003. Rapid Cenozoic glaciation of Antarctica induced by declining atmospheric CO₂. Nature 421 (6920), 245–249.
- Denton, G.H., Heusser, C.J., Lowel, T.V., Moreno, P.I., Andersen, B.G., Heusser, L.E., Schlühter, C., Marchant, D.R., 1999. Interhemispheric Linkage of Paleoclimate during the last Glaciation. Geogr. Ann. Ser. B 81 (2), 107–153.
- Doss, W., Marchitto, T.M., 2013. Glacial deep ocean sequestration of CO2 driven by the eastern equatorial Pacific biologic pump. Earth Planet. Sci. Lett. 377–378 (0), 43–54.
- Edmond, J.M., Huh, Y., 1997. Chemical weathering yields from basement and orogenic terrains in hot and cold climates. In: Ruddiman, W.F. (Ed.), Tectonic Uplift and Climate Change. Springer, US, Boston, MA, pp. 329–351.
- Emiliani, C., 1955. Pleistocene Temperatures. J. Geol. 63 (6), 538-578.
- Farrell, J.W., Prell, W.L., 1989. Climatic change and CaCO3 preservation: an 800,000 year bathymetric Reconstruction from the central equatorial Pacific Ocean. Paleoceanography 4 (4), 447–466.
- Foster, G.L., Vance, D., 2006. Negligible glacial-interglacial variation in continental chemical weathering rates. Nature 444 (7121), 918–921.
- Garity, M., Lund, D., 2024. Multi-Proxy evidence for Atlantic Meridional Overturning Circulation (AMOC) weakening during Deglaciations of the past 150,000 years. Paleoceanography and Paleoclimatology 39 (1) e2023PA004629.
- German, C.R., Baumberger, T., Lilley, M.D., Lupton, J.E., Noble, A.E., Saito, M., Thurber, A.R., Blackman, D.K., 2022. Hydrothermal exploration of the Southern Chile rise: sediment-hosted venting at the chile triple junction. Geochem. Geophys. Geosyst. 23 (3) e2021GC010317.
- Hansen, J.E., 2012. Paleoclimate implications for human-made climate change. In: Berger, F.M.A., Šijački, D. (Eds.), Climate Change: Inferences from Paleoclimate and Regional Aspects. Springer, pp. 21–48.
- Hays, J.D., Imbrie, J., Shackleton, N.J., 1976. Pacemaker of long-term climatic change. Trans. Am. Geophys. Union 57 (4), 259–259.
- Heaton, T.J., Köhler, P., Butzin, M., Bard, E., Reimer, R.W., Austin, W.E.N., Bronk Ramsey, C., Grootes, P.M., Hughen, K.A., Kromer, B., Reimer, P.J., Adkins, J., Burke, A., Cook, M.S., Olsen, J., Skinner, L.C., 2020. Marine20—the marine radiocarbon age calibration curve (0–55,000 cal BP). Radiocarbon 62 (4), 779–820.
- Hobart, B., Lisiecki, L.E., Rand, D., Lee, T., Lawrence, C.E., 2023. Late Pleistocene 100kyr glacial cycles paced by precession forcing of summer insolation. Nat. Geosci. 16, 717–722.
- Huybers, P., Langmuir, C., 2009. Feedback between deglaciation, volcanism, and atmospheric CO_2 . Earth Planet. Sci. Lett. 286 (3–4), 479–491.
- Huybers, P., Langmuir, C.H., 2017. Delayed CO_2 emissions from mid-ocean ridge volcanism as a possible cause of late-Pleistocene glacial cycles. Earth Planet. Sci. Lett. 457, 238–249.
- Imbrie, J., Imbrie, K.P., 1986. Ice Ages: Solving the Mystery. Harvard University Press. Inagaki, F., Kuypers, M.M.M., Tsunogai, U., Ishibashi, J.-I., Nakamura, K.-I., Treude, T., Ohkubo, S., Nakaseama, M., Gena, K., Chiba, H., Hirayama, H., Nunoura, T., Takai, K., Järgensen, B.B., Horikoshi, K., Boetius, A., 2006. Microbial community in a sediment-hosted CO₂ lake of the southern Okinawa Trough hydrothermal system. Proc. Natl. Acad. Sci. 103 (38), 14164–14169.
- Jacobel, A.W., Anderson, R.F., Jaccard, S.L., McManus, J.F., Pavia, F.J., Winckler, G., 2020. Deep Pacific storage of respired carbon during the last ice age: Perspectives

- from bottom water oxygen reconstructions. Quaternary Science Reviews 230 (106065), 1–20.
- Kawahata, H., 2005. Stable isotopic composition of two morphotypes of <i>Globigerinoides ruber</i> (white) in the subtropical gyre in the North Pacific. Paleontological Research 9 (1), 27–35.
- Kennett, J.P., Stott, L.D., 1991. Abrupt Deep-Sea Warming, Palaeoceanographic changes and Benthic Extinctions at the end of the Paleocene. Nature 353 (6341), 225–229.
- Key, R.M., Olsen, A., van Heuven, S., Lauvset, S.K., Velo, A., Lin, X., Schirnick, C., Kozyr, A., Tanhua, T., Hoppema, M., Jutterström, S., Steinfeldt, R., Jeansson, E., Ishii, M., Perez, F.F., Suzuki, T., 2015. Global Ocean Data Analysis Project, Version 2 (GLODAPv2), ORNL/CDIAC-162, NDP-093. Carbon Dioxide Information Analysis Center, Oak Ridge National Laboratory, US Department of Energy, Oak Ridge, Tennessee
- Köhler, P., Mulitza, S., 2023. No detectable influence of the carbonate ion effect on changes in stable carbon isotope ratios (d13C) of shallow dwelling planktic foraminifera over the past 160 kyr. Climate Past Discuss. 2023, 1–36.
- Köhler, P., van de Wal, R.S.W., 2020. Interglacials of the Quaternary defined by northern hemispheric land ice distribution outside of Greenland. Nat. Commun. 11 (1), 5124.
- Langner, M., Mulitza, S., 2019. Technical note: PaleoDataView a software toolbox for the collection, homogenization and visualization of marine proxy data. Clim. Past 15 (6), 2067–2072.
- Lasaga, A.C., Berner, R.A., Garrels, R.M., 1985. An Improved Geochemical Model of Atmospheric CO2 Fluctuations Over the Past 100 Million Years, The Carbon Cycle and Atmospheric CO2: Natural Variations Archean to Present, pp. 397–411.
- Lhardy, F., Bouttes, N., Roche, D.M., Abe-Ouchi, A., Chase, Z., Crichton, K.A., Ilyina, T., Ivanovic, R., Jochum, M., Kageyama, M., Kobayashi, H., Liu, B., Menviel, L., Muglia, J., Nuterman, R., Oka, A., Vettoretti, G., Yamamoto, A., 2021. A first Intercomparison of the simulated LGM Carbon results within PMIP-Carbon: Role of the Ocean Boundary Conditions. Paleoceanography and Paleoclimatology 36 (10) e2021PA004302.
- Li, G., Elderfield, H., 2013. Evolution of carbon cycle over the past 100 million years. Geochim. Cosmochim. Acta 103, 11–25.
- Lin, H.-L., Wang, W.-C., Hung, G.-W., 2004. Seasonal variation of planktonic foraminiferal isotopic composition from sediment traps in the South China Sea. Mar. Micropaleontol. 53 (3), 447–460.
- Lindsay, C.M., Lehman, S.J., Marchitto, T.M., Carriquiry, J.D., Ortiz, J.D., 2016. New constraints on deglacial marine radiocarbon anomalies from a depth transect near Baja CaliforniaT. Paleoceanography 31 (8), 1103–1116.
- Lisiecki, L.E., Raymo, M.E., 2005. A Pliocene-Pleistocene stack of 57 globally distributed benthic δ^{18} O records. Paleoceanography 20 (1) n/a-n/a.
- Lowell, T.V., Heusser, C.J., Andersen, B.G., Moreno, P.I., Hauser, A., Heusser, L.E., Schlüchter, C., Marchant, D.R., Denton, G.H., 1995. Interhemispheric Correlation of late Pleistocene Glacial events. Science 269 (5230), 1541–1549.
- Lund, D.C., 2013. Deep Pacific ventilation ages during the last deglaciation: evaluating the influence of diffusive mixing and source region reservoir age. Earth Planet. Sci. Lett. 381, 52–62.
- Lund, D.C., Asimow, P.D., 2011. Does sea level influence mid-ocean ridge magmatism on Milankovitch timescales? Geochem. Geophys. Geosyst. 12 (12).
- Lund, D.C., Mix, A.C., 1998. Millennial-scale deep water oscillations: Reflections of the North Atlantic in the deep Pacific from 10 to 60 ka. Paleoceanography 13 (1), 10–19.
- Lund, D.C., Mix, A.C., Southon, J., 2011. Increased ventilation age of the deep Northeast Pacific Ocean during the last deglaciation. Nat. Geosci. 4 (11), 771–774.
- Lund, D.C., Asimow, P.D., Farley, K.A., Rooney, T.O., Seeley, E., Jackson, E.W., Durham, Z.M., 2016. Enhanced East Pacific rise hydrothermal activity during the last two glacial terminations. Science 351 (6272), 478–482.
- Lupton, J., Butterfield, D., Lilley, M., Evans, L., Nakamura, K.-I., Chadwick Jr., W., Resing, J., Embley, R., Olson, E., Proskurowski, G., Baker, E., de Ronde, C., Roe, K., Greene, R., Lebon, G., Young, C., 2006. Submarine venting of liquid carbon dioxide on a Mariana Arc volcano. Geochem. Geophys. Geosyst. 7 (8).
- Lupton, J., Lilley, M., Butterfield, D., Evans, L., Embley, R., Massoth, G., Christenson, B., Nakamura, K., Schmidt, M., 2008. Venting of a separate CO₂-rich gas phase from submarine arc volcanoes: examples from the Mariana and Tonga-Kermadec arcs. J. Geophys. Res. 113.
- Luthi, D., Le Floch, M., Bereiter, B., Blunier, T., Barnola, J.-M., Siegenthaler, U., Raynaud, D., Jouzel, J., Fischer, H., Kawamura, K., Stocker, T.F., 2008. Highresolution carbon dioxide concentration record 650,000-800,000 years before present. Nature 453 (7193), 379–382.
- Marchitto, T.M., Lehman, S.J., Ortiz, J.D., Fluckiger, J., van Geen, A., 2007. Marine Radiocarbon evidence for the Mechanism of Deglacial Atmospheric CO₂ rise. Science 316 (5830), 1456–1459.
- Martin, J.H., 1990. Glacial-Interglacial CO_2 Change: the Iron Hypothesis. Paleoceanography 5, 1–13.
- Matsumoto, K., 2007. Radiocarbon-based circulation age of the world oceans. J. Geophys. Res. Oceans 112 (C9).
- Mekik, F.A., Anderson, R.F., Loubere, P., François, R., Richaud, M., 2012. The mystery of the missing deglacial carbonate preservation maximum. Quat. Sci. Rev. 39, 60–72.
- Members, P.P., 2012. Making sense of palaeoclimate sensitivity. Nature 491 (7426), 683–691.
- Menviel, L., Spence, P., Yu, J., Chamberlain, M.A., Matear, R.J., Meissner, K.J., England, M.H., 2018. Southern Hemisphere westerlies as a driver of the early deglacial atmospheric CO₂ rise. Nat. Commun. 9 (1), 2503.
- Mercer, J.H., 1984. Simultaneous Climatic Change in both Hemispheres and similar Bipolar Interglacial Warming: evidence and Implications. Climate Processes and Climate Sensitivity 307–313.

- Middleton, J.L., Langmuir, C.H., Mukhopadhyay, S., McManus, J.F., Mitrovica, J.X., 2016. Hydrothermal iron flux variability following rapid sea level changes. Geophys. Res. Lett. 43 (8), 3848–3856.
- Milanković, M., 1957. Astronomische Theorie der Klimaschwankungen.
- Misra, S., Froelich, P.N., 2012. Lithium Isotope history of Cenozoic Seawater: changes in Silicate Weathering and reverse Weathering. Science 335 (6070), 818–823.
- Muglia, J., Mulitza, S., Repschläger, J., Schmittner, A., Lembke-Jene, L., Lisiecki, L., Mix, A., Saraswat, R., Sikes, E., Waelbroeck, C., Gottschalk, J., Lippold, J., Lund, D., Martinez-Mendez, G., Michel, E., Muschitiello, F., Naik, S., Okazaki, Y., Stott, L., Voelker, A., Zhao, N., 2023. A global synthesis of high-resolution stable isotope data from benthic foraminifera of the last deglaciation. Scientific Data 10 (1), 131.
- Mulitza, S., Bickert, T., Bostock, H.C., Chiessi, C.M., Donner, B., Govin, A., Harada, N., Huang, E., Johnstone, H.J.H., Kuhnert, H., Langner, M., Lamy, F., Lembke-Jene, L., Lisiecki, L.E., Lynch-Stieglitz, J., Max, L., Mohtadi, M., Mollenhauer, G., Muglia, J., Nürnberg, D., Paul, A., Rühlemann, C., Repschläger, J., Saraswat, R., Schmittner, A., Sikes, E.L., Spielhagen, R.F., Tiedemann, R., 2021. World Atlas of Late Quaternary Foraminiferal Oxygen and Carbon Isotope Ratios (WA_Foraminiferal_Isotopes_2022). PANGAFA.
- Munhoven, G., 2002. Glacial–interglacial changes of continental weathering: estimates of the related CO₂ and HCO₃– flux variations and their uncertainties. Global Planet. Change 33 (1), 155–176.
- Nealson, K., 2006. Lakes of liquid CO_2 in the deep sea. Proc. Natl. Acad. Sci. 103 (38), 13903–13904.
- Numberger, L., Hemleben, C., Hoffmann, R., Mackensen, A., Schulz, H., Wunderlich, J.-M., Kucera, M., 2009. Habitats, abundance patterns and isotopic signals of morphotypes of the planktonic foraminifer Globigerinoides ruber (d'Orbigny) in the eastern Mediterranean Sea since the Marine Isotopic Stage 12. Marine Micropaleontology 73 (1), 90–104.
- Okazaki, Y., Sagawa, T., Asahi, H., Horikawa, K., Onodera, J., 2012. Ventilation changes in the western North Pacific since the last glacial period. Clim. Past 8 (1), 17–24.
- Peterson, C.D., Lisiecki, L.E., Stern, J.V., 2014. Deglacial whole-ocean δ13C change estimated from 480 benthic foraminiferal records. Paleoceanography 29 (6), 549–563.
- Prend, C.J., Gray, A.R., Talley, L.D., Gille, S.T., Haumann, F.A., Johnson, K.S., Riser, S.C., Rosso, I., Sauvé, J., Sarmiento, J.L., 2022. Indo-pacific sector dominates southern ocean carbon outgassing. Global Biogeochem. Cycles 36 (7) e2021GB007226.
- Putnam, A.E., Schaefer, J.M., Denton, G.H., Barrell, D.J.A., Birkel, S.D., Andersen, B.G., Kaplan, M.R., Finkel, R.C., Schwartz, R., Doughty, A.M., 2013. The last Glacial Maximum at 44°S documented by a ¹⁰Be moraine chronology at Lake Ohau, Southern Alps of New Zealand. Quaternary Science Reviews 62, 114–141.
- Rafter, P.A., Carriquiry, J.D., Herguera, J.-C., Hain, M.P., Solomon, E.A., Southon, J.R., 2019. Anomalous > 2000-year-old surface ocean radiocarbon age as evidence for deglacial geologic carbon release. Geophysical Research Letters 46 (23), 13950–13960.
- Rafter, P.A., Gray, W.R., Hines, S.K.V., Burke, A., Costa, K.M., Gottschalk, J., Hain, M.P., Rae, J.W.B., Southon, J.R., Walczak, M.H., Yu, J., Adkins, J.F., DeVries, T., 2022. Global reorganization of deep-sea circulation and carbon storage after the last ice age. Science Advances 8 (46), eabo5434.
- Raymo, M.E., Ruddiman, W.F., 1992. Tectonic forcing of late Cenozoic climate. Nature 359 (6391), 117–122.
- Raymo, M.E., Ruddiman, W.F., Froelich, P.N., 1988. Influence of late Cenozoic mountain building on ocean geochemical cycles. Geology 16 (7), 649–653.
- Rohling, E.J., Grant, K., Bolshaw, M., Roberts, A.P., Siddall, M., Hemleben, C., Kucera, M., 2009. Antarctic temperature and global sea level closely coupled over the past five glacial cycles. Nat. Geosci. 2 (7), 500–504.
- Ronge, T.A., Tiedemann, R., Lamy, F., Kohler, P., Alloway, B.V., De Pol-Holz, R., Pahnke, K., Southon, J., Wacker, L., 2016. Radiocarbon constraints on the extent and evolution of the South Pacific glacial carbon pool. Nature Communications 7.
- Ronge, T.A., Sarnthein, M., Roberts, J., Lamy, F., Tiedemann, R., 2019. East Pacific rise Core PS75/059-2: Glacial-to-Deglacial Stratigraphy Revisited. Paleoceanography and Paleoclimatology 34 (4), 432–435.
- Schmittner, A., Bostock, H.C., Cartapanis, O., Curry, W.B., Filipsson, H.L., Galbraith, E. D., Gottschalk, J., Herguera, J.C., Hoogakker, B., Jaccard, S.L., Lisiecki, L.E., Lund, D.C., Martínez-Méndez, G., Lynch-Stieglitz, J., Mackensen, A., Michel, E., Mix, A.C., Oppo, D.W., Peterson, C.D., Repschläger, J., Sikes, E.L., Spero, H.J., Waelbroeck, C., 2017. Calibration of the carbon isotope composition (8¹³C) of benthic foraminifera. Paleoceanography 32 (6), 512–530.
- Sexton, P.F., Barker, S., 2012. Onset of 'Pacific-style' deep-sea sedimentary carbonate cycles at the mid-Pleistocene transition. Earth Planet. Sci. Lett. 321-322, 81–94.
- Siani, G., Michel, E., De Pol-Holz, R., DeVries, T., Lamy, F., Carel, M., Isguder, G., Dewilde, F., Lourantou, A., 2013. Carbon isotope records reveal precise timing of enhanced Southern Ocean upwelling during the last deglaciation. Nat. Commun. 4.
- Sigman, D.M., Hain, M.P., Haug, G.H., 2010. The polar ocean and glacial cycles in atmospheric $\rm CO_2$ concentration. Nature 466 (7302), 47–55.
- Shackleton, N.J., 1977. Carbon-13 in Uvigerina: Tropical rain forest history and the equatorial Pacific carbonate dissolution cycle. The fate of fossil fuel ${\rm CO_2}$ in the. oceans 401–428.
- Sikes, E.L., Samson, C.R., Guilderson, T.P., Howard, W.R., 2000. Old radiocarbon ages in the Southwest Pacific Ocean during the last glacial period and deglaciation. Nature 405 (6786), 555–559.
- Skinner, L., McCave, I.N., Carter, L., Fallon, S., Scrivner, A.E., Primeau, F., 2015.
 Reduced ventilation and enhanced magnitude of the deep Pacific carbon pool during the last glacial period. Earth Planet. Sci. Lett. 411 (0), 45–52.
- Skinner, L., Primeau, F., Jeltsch-Thömmes, A., Joos, F., Köhler, P., Bard, E., 2023. Rejuvenating the ocean: mean ocean radiocarbon, CO₂ release, and radiocarbon budget closure across the last deglaciation. Clim. Past 19 (11), 2177–2202.

- Spero, H.J., Mielke, K.M., Kalve, E.M., Lea, D.W., Pak, D.K., 2003. Multispecies approach to reconstructing eastern equatorial Pacific thermocline hydrography during the past 360 kyr. Paleoceanography 18 (1).
- Stott, L.D., 2020. Assessing the stratigraphic integrity of planktic and benthic 14 C records in the western Pacific for Δ^{14} C reconstructions at the last glacial termination. Radiocarbon 62 (5), 1389–1402.
- Stott, L.D., 2023. How old is too old? Implications of averaging ¹⁴C-based estimates of ventilation age to assess the Pacific Ocean's role in sequestering CO₂ in the past. Quaternary Science Reviews 310, 108122.
- Stott, L., Timmermann, A., 2011. Hypothesized Link between Glacial/Interglacial Atmospheric CO₂ Cycles and Storage/Release CO₂-Rich Fluids from the Deep Sea., Geophysical Monograph Series: Understanding the Causes, Mechanisms and Extent of the Abrupt Climate Change. American Geophysical Union.
- Stott, L., Southon, J., Timmermann, A., Koutavas, A., 2009. Radiocarbon age anomaly at intermediate water depth in the Pacific Ocean during the last deglaciation. Paleoceanography 24 (2).
- Stott, L., Davy, B., Shao, J., Coffin, R., Pecher, I., Neil, H., Rose, P., Bialas, J., 2019a. CO₂ Release from Pockmarks on the Chatham Rise-Bounty Trough at the Glacial termination. Paleoceanography and Paleoclimatology 34 (11), 1726–1743.
- Stott, L.D., Harazin, K.M., Quintana Krupinski, N.B., 2019b. Hydrothermal carbon release to the ocean and atmosphere from the eastern equatorial Pacific during the last glacial termination. Environ. Res. Lett. 14 (2), 025007.
- Stott, L.D., Shao, J., Yu, J., Harazin, K.M., 2021. Evaluating the Glacial-Deglacial Carbon Respiration and Ventilation Change Hypothesis as a Mechanism for changing Atmospheric CO₂. Geophys. Res. Lett. 48 (3) e2020GL091296.

- Toggweiler, J.R., Gnanadesikan, A., Carson, S., Murnane, R., Sarmiento, J.L., 2003a. Representation of the Carbon Cycle in Box Models and GCMs: 1, 17. Solubility pump. Global Biogeochem. Cycles.
- Toggweiler, J.R., Murnane, R., Carson, S., Gnanadesikan, A., Sarmiento, J.L., 2003b.
 Representation of the Carbon Cycle in Box Models and GCMs, 2, 17. Organic pump.
 Global Biogeochem. Cycles.
- Urey, H.C., 1952. On the early Chemical history of the Earth and the Origin of Life. Proc. Natl. Acad. Sci. 38 (4), 351–363.
- Walker, J.C.G., Hays, P.B., Kasting, J.F., 1981. A negative feedback mechanism for the long-term stabilization of the earth's surface temperature. J. Geophys. Res. 86, 9776.
- Wallmann, K., 2001. Controls on the cretaceous and cenozoic evolution of seawater composition, atmospheric CO₂ and climate. Geochim. Cosmochim. Acta 65 (18), 3005–3025.
- Wallmann, K., Schneider, B., Sarnthein, M., 2016. Effects of eustatic sea-level change, ocean dynamics, and nutrient utilization on atmospheric pCO₂ and seawater composition over the last 130 000 years: a model study. Clim. Past 12 (2), 339–375.
- Yu, J., Broecker, W.S., Elderfield, H., Jin, Z., McManus, J., Zhang, F., 2010. Loss of Carbon from the Deep Sea since the last Glacial Maximum. Science 330 (6007), 1084–1087.
- Yu, J., Thornalley, D.J.R., Rae, J.W.B., McCave, N.I., 2013. Calibration and application of B/Ca, Cd/Ca, and δ^{11} B in Neogloboquadrina pachyderma (sinistral) to constrain CO₂ uptake in the subpolar North Atlanti. Paleoceanography 28 (2), 237–252.
- Zachos, J., Pagani, M., Sloan, L., Thomas, E., Billups, K., 2001. Trends, Rhythms, and Aberrations in Global climate 65 Ma to present. Science 292 (5517), 686–693.
- Zeebe, R.E., Caldeira, K., 2008. Close mass balance of long-term carbon fluxes from icecore CO2 and ocean chemistry records. Nat. Geosci. 1 (5), 312–315.